



**Calhoun: The NPS Institutional Archive**  
**DSpace Repository**

---

Theses and Dissertations

Thesis and Dissertation Collection

---

1976

Laser doppler anemometer measurement and analytical comparison of flow around a cylinder at low Reynolds number.

Wanner, Terry Scott

Monterey, California. Naval Postgraduate School

---

<http://hdl.handle.net/10945/17832>

*Downloaded from NPS Archive: Calhoun*



Calhoun is a project of the Dudley Knox Library at NPS, furthering the precepts and goals of open government and government transparency. All information contained herein has been approved for release by the NPS Public Affairs Officer.

**Dudley Knox Library / Naval Postgraduate School**  
**411 Dyer Road / 1 University Circle**  
**Monterey, California USA 93943**

<http://www.nps.edu/library>

LASER DOPPLER ANEMOMETER MEASUREMENT AND  
ANALYTICAL COMPARISON OF FLOW AROUND A  
CYLINDER AT LOW REYNOLDS NUMBER

Terry Scott Wanner

# NAVAL POSTGRADUATE SCHOOL

## Monterey, California



# THESIS

Laser Doppler Anemometer Measurement and  
Analytical Comparison of Flow Around a  
Cylinder at Low Reynolds Number

by  
Terry Scott Wanner

March 1976

Thesis Advisor:

D. J. Collins

Approved for public release; distribution unlimited.

T175040

SECURITY CLASSIFICATION OF THIS PAGE (When Data Entered)

## REPORT DOCUMENTATION PAGE

READ INSTRUCTIONS  
BEFORE COMPLETING FORM

1. REPORT NUMBER		2. GOVT ACCESSION NO.	3. RECIPIENT'S CATALOG NUMBER
4. TITLE (and Subtitle) Laser Doppler Anemometer Measurement and Analytical Comparison of Flow Around a Cylinder at Low Reynolds Number		5. TYPE OF REPORT & PERIOD COVERED Master's Thesis March 1976	
7. AUTHOR(s)  Terry Scott Wanner		6. PERFORMING ORG. REPORT NUMBER	
9. PERFORMING ORGANIZATION NAME AND ADDRESS Naval Postgraduate School Monterey, California 93940		8. CONTRACT OR GRANT NUMBER(s)	
11. CONTROLLING OFFICE NAME AND ADDRESS Naval Postgraduate School Monterey, California 93940		10. PROGRAM ELEMENT, PROJECT, TASK AREA & WORK UNIT NUMBERS	
12. REPORT DATE March 1976		13. NUMBER OF PAGES 61	
14. MONITORING AGENCY NAME & ADDRESS (if different from Controlling Office) Naval Postgraduate School Monterey, California 93940		15. SECURITY CLASS. (of this report) Unclassified	
16. DISTRIBUTION STATEMENT (of this Report)  Approved for public release; distribution unlimited.		15a. DECLASSIFICATION/DOWNGRADING SCHEDULE	
17. DISTRIBUTION STATEMENT (of the abstract entered in Block 20, if different from Report)			
18. SUPPLEMENTARY NOTES			
19. KEY WORDS (Continue on reverse side if necessary and identify by block number)  LDV Laser Doppler Velocimeter			
20. ABSTRACT (Continue on reverse side if necessary and identify by block number)  In this study, the flow characteristics of air around a circular cylinder were determined by two means: by analytical solution of the Navier-Stokes equations, and actual measurement of the flow itself. A DISA LD 5586 laser doppler anemometer system was employed to measure normal (v) and parallel (u) velocity components of a laminar flow regime about a three-sixteenths inch diameter cylinder mounted in a 32 x 45 inch wind tunnel (Reynolds number approximately 40).			

A finite element grid was constructed using triangular elements which encompassed the upper half-cylinder. Flow measurements using the laser velocimeter were confined to this region of interest.

Theory was compared against experimental results, and the feasibility of the utilization of this particular type of laser anemometer was evaluated.

Laser Doppler Anemometer Measurement and Analytical  
Comparison of Flow Around a Cylinder  
at Low Reynolds Number

by

Terry Scott Wanner  
Lieutenant, United States Navy  
B.S., United States Naval Academy, 1969

Submitted in partial fulfillment of the  
requirements for the degree of

MASTER OF SCIENCE IN AERONAUTICAL ENGINEERING

from the

NAVAL POSTGRADUATE SCHOOL  
March 1976



I.        ABSTRACT

In this study, the flow characteristics of air around a circular cylinder were determined by two means: by analytical solution of the Navier-Stokes equations, and actual measurement of the flow itself. A DISA LD 5586 laser doppler anemometer system was employed to measure normal (v) and parallel (u) velocity components of a laminar flow regime about a three-sixteenths inch diameter cylinder mounted in a 32 x 45 inch wind tunnel (Reynolds number approximately 40).

A finite element grid was constructed using triangular elements which encompassed the upper half-cylinder. Flow measurements using the laser velocimeter were confined to this region of interest.

Theory was compared against experimental results, and the feasibility of the utilization of this particular type of laser anemometer was evaluated.

## TABLE OF CONTENTS

I.	ABSTRACT .....	3
II.	DESCRIPTION OF LASER ANEMOMETER .....	6
III.	ANALYTICAL DERIVATION .....	14
IV.	DESCRIPTION OF EXPERIMENT .....	22
V.	DESCRIPTION OF COMPUTER PROGRAM .....	28
VI.	ANALYSIS OF RESULTS .....	31
	A. ERROR ANALYSIS .....	34
VII.	CONCLUSION .....	35
	APPENDIX A LDV data .....	36
	COMPUTER PROGRAM .....	38
	BIBLIOGRAPHY .....	61



## II. DESCRIPTION OF LASER ANEMOMETER

A basic laser anemometer is comprised of four primary elements:

- (1) a coherent light source
- (2) optics
- (3) signal converter (photomultiplier tube)
- (4) signal processor/display

The principle of the laser anemometer is to create a grid pattern and measure the speed with which a particle in a fluid free stream passes through the grid. The following assumptions were taken into consideration:

- (1) particles injected into the free stream are small enough to faithfully follow stream lines of the flow, thus by measuring particle characteristics, we are actually measuring the medium's characteristics. This is easily achieved by use of particles which are on the order of a few microns in diameter.
- (2) particle generation results in a consistent particle size, or at least a majority of the particles are within a specified range of sizes. For example, DOP (di-2-ethylhexyl phthalate) particle generators produce particles with a mean diameter of 0.75 microns and burning turbine oil produces particles on the order of 4-6 microns (from electron microscope).

A laser is incorporated because of its coherency and power. The aforementioned grid is in reality the result of two coherent beams interfering with themselves (Fig. 1). The optics produce the beam pair by conventional splitting and focusing. Because the laser beam intensity is of a Gaussian distribution the grid created by constructive and destructive interference is not uniform over the entire focal volume. The fringes created on the outer portions of the horizontal axis are not perfectly formed because of slightly different intensities in that area. The main portion of the interference grid is uniform and, most importantly, the fringe spacing ( $D_f$ ) is determined only by the laser wavelength ( $\lambda$ ) and the half angle of the beam pair convergence ( $\theta/2$ ).

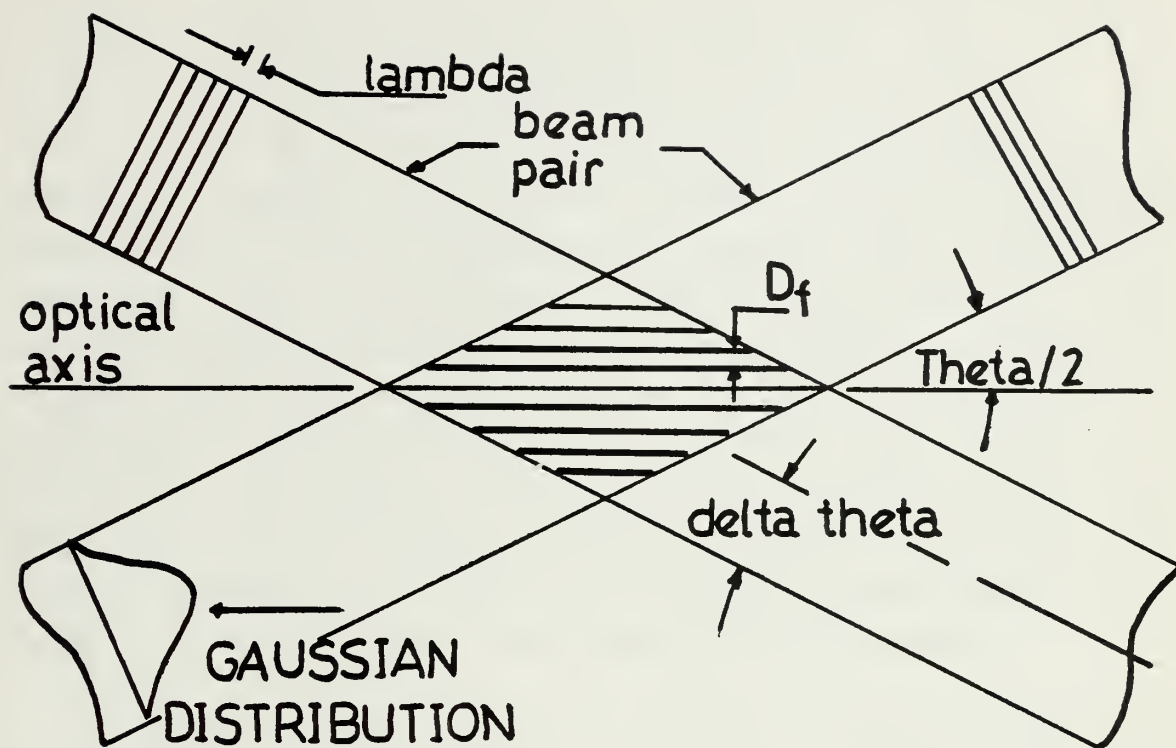
$$D_f = \lambda / (2 \sin(\theta/2))$$

The number of fringes ( $N_f$ ) may also be computed, provided the beam focusing convergence angle ( $\Delta \theta$ ) is known, by the relation:

$$N_f = 8 \tan(\theta/2) / (\pi \Delta \theta)$$

The number of fringes is important only to ensure that the signal processing apparatus will receive enough information to make possible further data reduction. If an insufficient number of fringes exists, not enough signal will be available for velocity determination.

Solid particles with a mean diameter which is less than half the fringe spacing are introduced into the free stream



## FRINGE PATTERN GEOMETRY

Figure 1

of the fluid to be measured. When the particle is small compared to the fringe spacing the scattered light exhibits essentially 100% modulation, while particles equal to the fringe spacing produce negligible modulation[Ref. 2]. The particles may be produced by atomization of water, dop-air reaction, burning oil, smoke bombs, or may be bought commercially, as e.g. polystyrene spheres and some solid chemicals such as zinc oxide. Choice of the particle to be used is normally dictated by the fringe spacing in the focal volume, and the nature of the medium to be measured. Regardless of choice, the particle must be small enough to follow the streamlines as closely as possible, because the laser anemometer actually measures the particle velocity and unless the particle's motion is a true representation of the fluid velocity, pertinent data may not be obtained.

Inside the measuring (or focal) volume, bands of darkness and brightness exist due to the interference of the two beams. Particles entering the focal volume will alternately scatter light as they pass through regions of constructive interference ( typical focal volume dimensions are 300 microns wide by 4 millimeters long and contain approximately 64 fringes). A photomultiplier tube located on the optical axis and focused into the measuring volume receives this scattered light and converts what appears to be a modulated light signal into a series of voltage pulses. Each voltage pulse correlates to a particle crossing one fringe. Because the spacing of the fringes is known, the frequency of the voltage pulse train may be equated to the velocity of the particle by the following relationship:

$$f = V_0 / D_f = 2 * V_0 * \sin(\Theta/2) / \lambda$$

where  $D_f$  is the fringe spacing and  $V_0$  is the velocity of the

particle. Now the processor is left with a fairly simple task of counting the frequency and multiplying it by a calibration factor, which is, in essence, a fringe spacing parameter to arrive at a velocity.

As long as we are assured that only one particle is in the measuring volume at one time, the apparatus will operate correctly, but this is an unrealistic assumption. In order to achieve such a situation, the seeding density of the particles would be exceptionally sparse and the resulting data rate would be so slow as to preclude timely data reduction. To overcome this obstacle, a validation circuit is incorporated into the counter/processor. When a particle crosses a fringe spacing, two counters are triggered. One measures the time duration for five fringe crossings and holds this information. The second counter continues to measure the time for a total of eight fringe crossings. The time of the first counter is then compared with that of the second counter, and if the first time is indeed five-eighths of the second time (within specified limits, i.e., comp. accuracy) a validation gate is opened and the resultant frequency is then stored into an ensemble cell. The ensemble cell is adjustable to hold various numbers of counts and average them for the final velocity display. The final displayed velocity then is that component of fluid velocity which is perpendicular to the optical axis and contained in the same plane as the beam pair (Fig. 2).

The anemometer may be operated in three modes: reference beam, forward scatter, and back scatter. The last two modes are most frequently employed and are described here:

Forward scatter mode: in this mode, the photomultiplier tube is located on the optical axis and focused in a direction directly opposed to the direction of the emerging beam pairs. This mode offers the strongest attainable



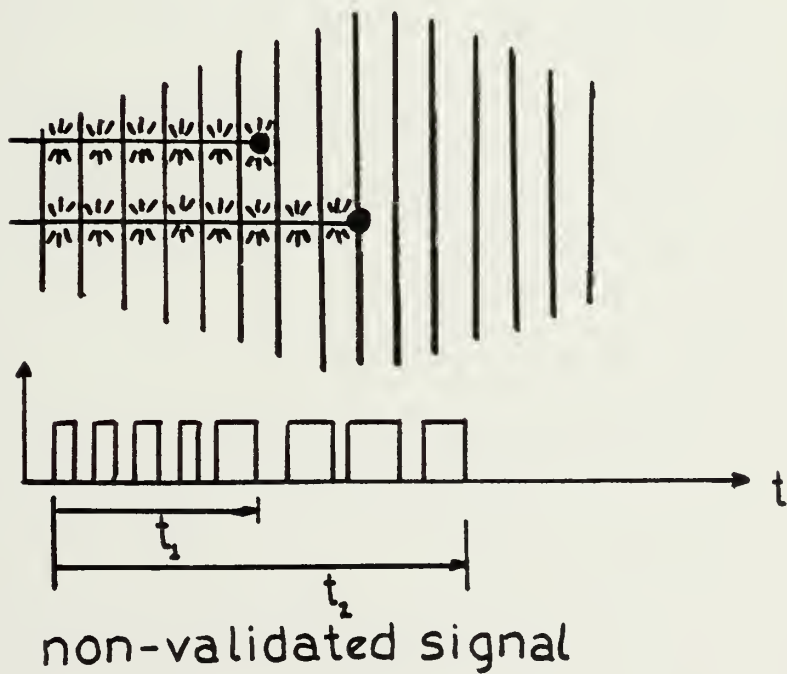
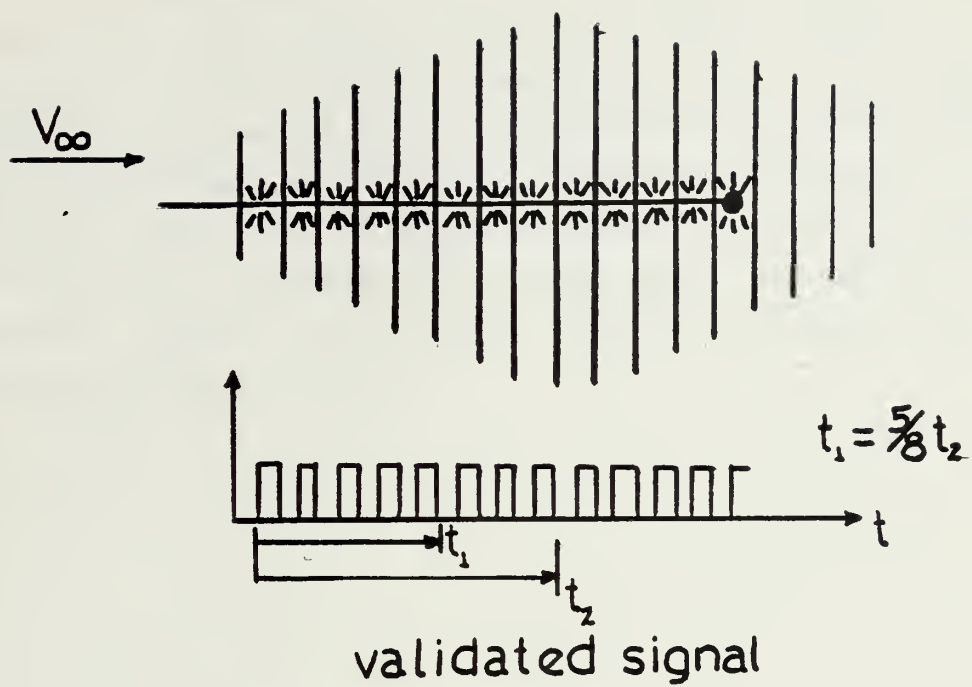
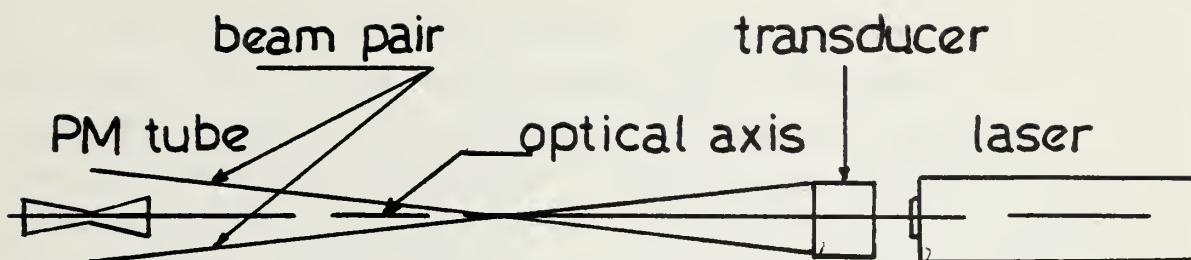


Figure 2

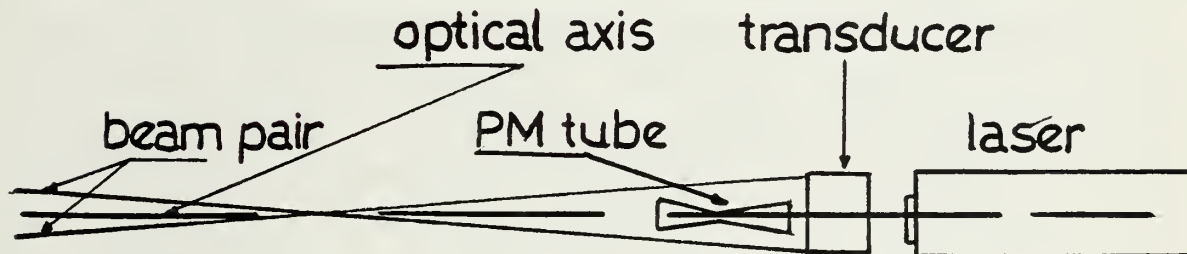
signal.

Back scatter mode: again the photomultiplier tube is mounted on the optical axis, but now it is aligned in the direction of the emerging beam pairs. This mode affords the ability to measure fluid velocities in confined spaces or in situations where the detector cannot be mounted in forward scatter, such as in measuring velocities in a compressor. Additionally, operation in this mode requires a higher powered laser due to the reduced intensity of back scattered light (Fig. 3).





LDV FORWARD SCATTER MODE



LDV BACK SCATTER MODE

Figure 3

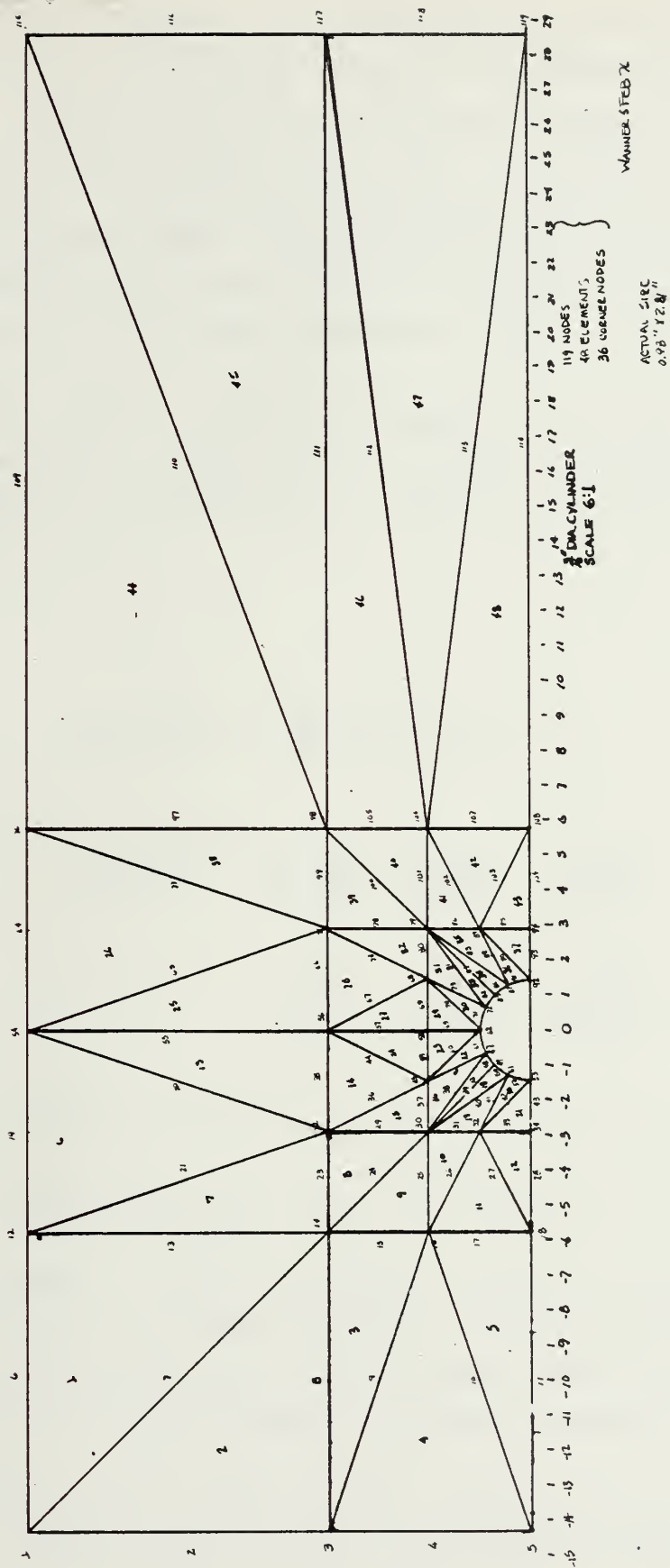
### III ANALYTICAL DERIVATION

The finite element method is a numerical analysis technique for obtaining approximate solutions to a wide variety of engineering problems. It offers a means to solve complex continuum problems by sub-dividing them into simpler interrelated problems. The nature of this engineering problem does not readily lend itself to a closed form solution. Therefore a numerical solution is dictated.

The method of finite elements is well employed where there are irregular geometries or unusual specifications of boundary conditions. The method gives a piecewise approximation to the governing equations. Figure 4 shows the finite element grid employed in this flow problem. Approximating functions (interpolation functions) are defined in terms of the values of the field variables at the nodes. For the finite element representation, the nodal values of the field variables become the new unknowns and, once found, the interpolation functions define the field variable throughout the field of elements. The degree of the interpolation polynomials is governed by the number of nodes per element and dictated by the order of the governing equations.

The basic principle of the finite element method is to divide the solution domain into a finite number of subdomains (elements) which are connected only at node points. Interpolation polynomials are created for each element and a collection of interpolation functions over the whole solution domain provide a piecewise approximation to the field variable.

Introduction of generalizations facilitate direct derivation of finite element equations from governing differential equations. The method of weighted residuals



Finite element grid

Figure 4

(Galerkin's Method) is a technique for obtaining approximate solutions to non-linear partial differential equations. We first assume the general function behavior of the dependent field variable in some way so as to approximately satisfy the given differential equations and boundary conditions. After applying this approximation to the original equations, some error will result, which we desire to minimize or drive to zero over the entire solution domain.

The basic set of differential equations governing the problem from a velocity and pressure formulation approach are (after linearization by approximating non-linear viscous terms  $u_n, v_n$ ):

$$\text{continuity} \quad \frac{\partial u}{\partial x} + \frac{\partial v}{\partial y} = 0$$

$$\text{momentum} \quad u_n \frac{\partial u}{\partial x} + v_n \frac{\partial u}{\partial y} = -\frac{1}{\rho} \frac{\partial P}{\partial x} + \nu \nabla^2 u$$

$$u_n \frac{\partial v}{\partial x} + v_n \frac{\partial v}{\partial y} = -\frac{1}{\rho} \frac{\partial P}{\partial y} + \nu \nabla^2 v$$

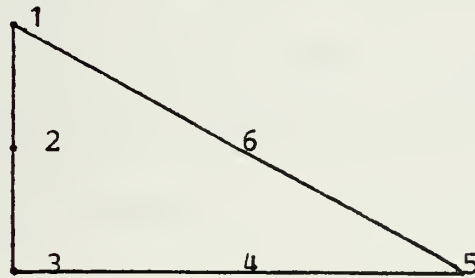
$u_n, v_n$ , and  $P_n$  are approximate solutions to the flow problem

and may be visualized as the  $n^{\text{th}}$  iteration of the procedure of solution. These equations used in formulation of the problem are by no means unique. Stream functions and stream function with vorticity formulations have also been employed to establish finite element solution procedures.

Inasmuch as the velocity terms are of second order, a second order interpolation polynomial must be used to

calculate these unknowns. The pressure terms are of first order and hence require only first order interpolation.

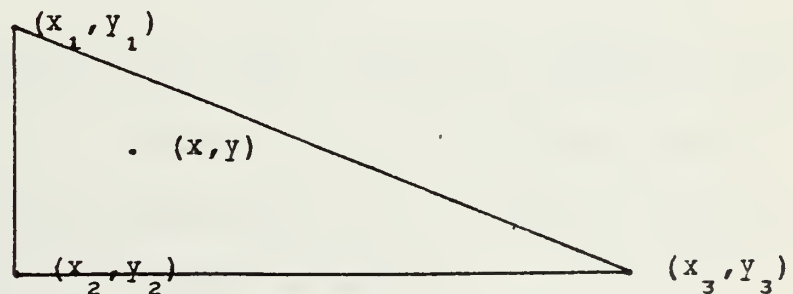
The basic element chosen for this solution was the triangle and, in a localized scheme, is visualized as follows:



Nodes 2, 4 and 6 lie equidistant between their respective corner nodes.

Nodes 1, 3, and 5 are referred to as corner nodes and are the basis for the linear interpolation polynomials derived for the pressure terms. For any triangular element, the corner nodes are described by their Cartesian coordinates  $x_i, y_i$ .

Consider the following local element:



The coordinates of node one are  $x_1, y_1$ ; node two  $x_2, y_2$ ; etc. and the interior point  $(x, y)$  may be described as a linear combination of the three corner nodes:

$$x = L_1 x_1 + L_2 x_2 + L_3 x_3$$

$$y = L_1 y_1 + L_2 y_2 + L_3 y_3$$

where  $L_i$  is the natural coordinate (interpolation polynomial, here linear) or weighting function which relates the coordinates of the corner nodes to any interior node.  $L_i$  has a value of one at the point  $x_i, y_i$  and is zero at the other two nodes of the element.

The  $L_i$ 's expressed as linear functions of the Cartesian coordinates then are

$$L_1(x, y) = \frac{1}{2\Delta} (a_1 + b_1 x + c_1 y)$$

$$L_2(x, y) = \frac{1}{2\Delta} (a_2 + b_2 x + c_2 y)$$

$$L_3(x, y) = \frac{1}{2\Delta} (a_3 + b_3 x + c_3 y)$$

$$\text{where } 2\Delta = \begin{vmatrix} 1 & x_1 & y_1 \\ 1 & x_2 & y_2 \\ 1 & x_3 & y_3 \end{vmatrix}$$

which is equal to the area of the triangular element and  $a_1 = x_2 y_3 - x_3 y_2$ ,  $b_1 = y_2 - y_3$ , and  $c_1 = y_1 - y_2$ , the determinants of the minors corresponding coefficients  $a_1$ ,  $b_1$ , or  $c_1$ , and the other coefficients are similarly computed.

For the velocity terms, second order interpolation polynomials are indicated, while the pressure terms remain first order. Hence the introduction of more nodes (6) will result in a new set of weighting functions which may also be



expressed in terms of the natural coordinate interpolation polynomials:

$$N_1 = 2L_1^2 - L_1$$

$$N_2 = 4L_1 L_2$$

$$N_3 = 2L_2^2 - L_2$$

$$N_4 = 4L_2 L_3$$

$$N_5 = 2L_3^2 - L_3$$

$$N_6 = 4L_1 L_3$$

$$N_i^P = L_i$$

$$u^e = \sum_i^6 N_i u_i$$

$$v^e = \sum_i^6 N_i v_i$$

$$P^e = \sum_i^3 N_i^P P_i \quad (xxxx)$$

Application of Galerkin's Method to the governing equations results in the following integral expressions:

$$-\int_{\Omega} N_i \left( u_n \frac{\partial u}{\partial x} + v_n \frac{\partial u}{\partial y} + \frac{1}{\rho} \frac{\partial P}{\partial x} - \nu \nabla^2 u \right) d\Omega = 0$$

$$-\int_{\Omega} N_i \left( u_n \frac{\partial v}{\partial x} + v_n \frac{\partial v}{\partial y} + \frac{1}{\rho} \frac{\partial P}{\partial y} - \nu \nabla^2 v \right) d\Omega = 0$$

$$\int_{\Omega} N_i^{(P)} \left( \frac{\partial u}{\partial x} + \frac{\partial v}{\partial y} \right) d\Omega = 0$$

here  $\Omega$  implies "over the area of the triangle".

Then we may make the substitution of the field variable in terms of x and y into terms of  $L_i$ .

e.g.: given  $u(x,y) \Leftrightarrow u(L_i)$

then  $\frac{\partial u}{\partial x} = u^e \frac{\partial N_i}{\partial L_i} \frac{\partial L_i}{\partial x}$

where  $\frac{\partial L_i}{\partial x} = \frac{b_i}{2\Delta}$

and a similar procedure for  $\frac{\partial u}{\partial y} = u^e \frac{\partial N_i}{\partial L_i} \frac{\partial L_i}{\partial y}$



where  $\frac{\partial \bar{c}_i}{\partial y} = \frac{c_i}{2\Delta}$

Substitution of equations (xxxx) into  $u^e$ ,  $v^e$  and  $P^e$  and application of the above chain rule allows integration by parts:

$$K_1 = \int \left[ \frac{\mu}{\rho} \left( \frac{\partial N_i}{\partial x} \frac{\partial N_j}{\partial x} + \frac{\partial N_i}{\partial y} \frac{\partial N_j}{\partial y} \right) - u^{(e)} N_i \frac{\partial N_j}{\partial x} - v^{(e)} N_i \frac{\partial N_j}{\partial y} \right] dx dy$$

$$K_2 = - \int N_j^{(r)} \frac{\partial N_i}{\partial x} dx dy$$

$$K_3 = - \int N_j^{(m)} \frac{\partial N_i}{\partial y} dx dy$$

The evaluated integral expressions then form the influence matrix as follows:

$$\begin{bmatrix} K_1 & 0 & K_2 \\ 0 & K_1 & K_3 \\ K_2 & K_3 & 0 \end{bmatrix}$$

Specification of the field variables or right hand sides of the matrix equation then provides a defined problem:

$$[TM] \cdot [T] = [Q]$$

Additionally, evaluation of the integral expressions yields boundary terms which must be computed for nodes which lie on the boundary of the control surface:

$$R_1 = \int N_i X^* ds \quad R_2 = \int N_i Y^* ds$$

$$\text{where } X^* = \mu \nabla u^{(e)} \cdot \hat{n} - \hat{n}_x P^{(e)} \quad \text{and} \quad Y^* = \mu \nabla v^{(e)} \cdot \hat{n} - \hat{n}_y P^{(e)}$$

It should be noted that along vertical boundaries there is

no outward pointing normal  $\hat{n}_y$  and similarly along horizontal boundaries no  $\hat{n}_x$  exists, and furthermore these terms are not computed where  $u$  and  $v$  are specified. Additionally, it was assumed that along the left-and right-hand side and upper boundaries  $\partial u / \partial x$  and  $\partial v / \partial y$  were identically equal to zero because these boundaries were placed at five or more characteristic lengths (diameters) from the cylinder and considered to be outside the realm of influence of the flow about the cylinder.

The terms comprising  $K_1$ ,  $K_2$  and  $K_3$  are entered element by element into the main program in steps FLU02080 through QZ00170. Then each element's matrix is compiled into the field matrix (comprised of all elemental matrices) and is solved iteratively to output the horizontal velocity component  $u$ , the vertical component  $v$ , and the pressure  $P$  at every node in the field.

#### IV. DESCRIPTION OF EXPERIMENT

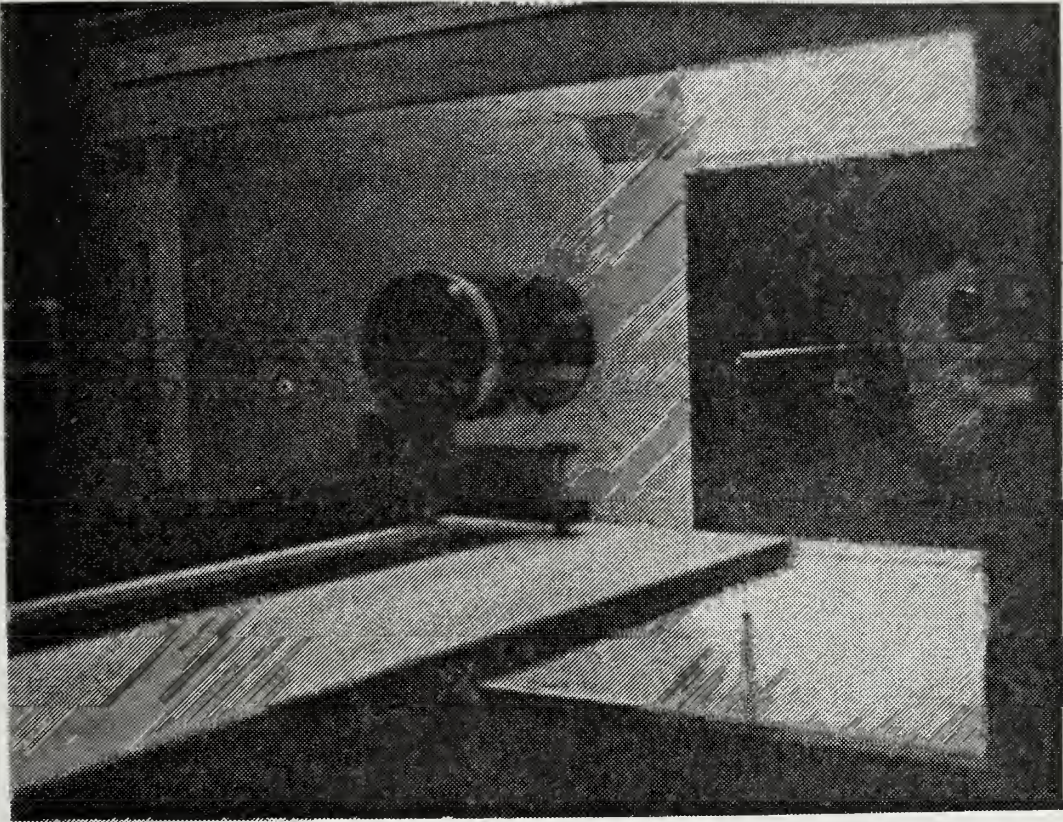
A right-angled, three-sixteenths inch cylinder made of stainless steel was mounted in an AEROLAB series 90 32x45 inch low speed wind tunnel through the floor of the test section (Fig. 5). The portion of the rod protruding down through the test section was mounted on a two-degree-of-freedom, micrometer controlled bed which allowed the rod to be maneuvered in the vertical plane parallel to the flow direction. This scheme enabled the laser velocimeter and photomultiplier tube to be mounted, aligned and left undisturbed for the entire period during which data were taken. The bed was positioned to read locations in the control volume which directly coincided with the location of the nodes in the finite element mesh (Fig. 6).

In the interest of precluding as many opportunities for error as possible, all  $u$  velocity components were first read and then components in a forty-five degree position were taken thus necessitating only one re-orientation of the beam pairs.

The plexiglass window prefacing the optics transducer of the test section had one-quarter inch holes drilled into it to allow the beam pairs to pass unimpeded, thereby minimizing distortion of the focal volume fringe pattern. The photomultiplier tube was likewise accommodated through the far window.

The seeding mechanism employed zinc-hexachloroethane based (non-toxic) white smoke bombs. The nature of the closed return wind tunnel permitted continuous measurement without interruption for re-seeding of the flow. By means of electron microscopy, the average size of the smoke particles was determined to be on the order of two microns (Fig. 7).

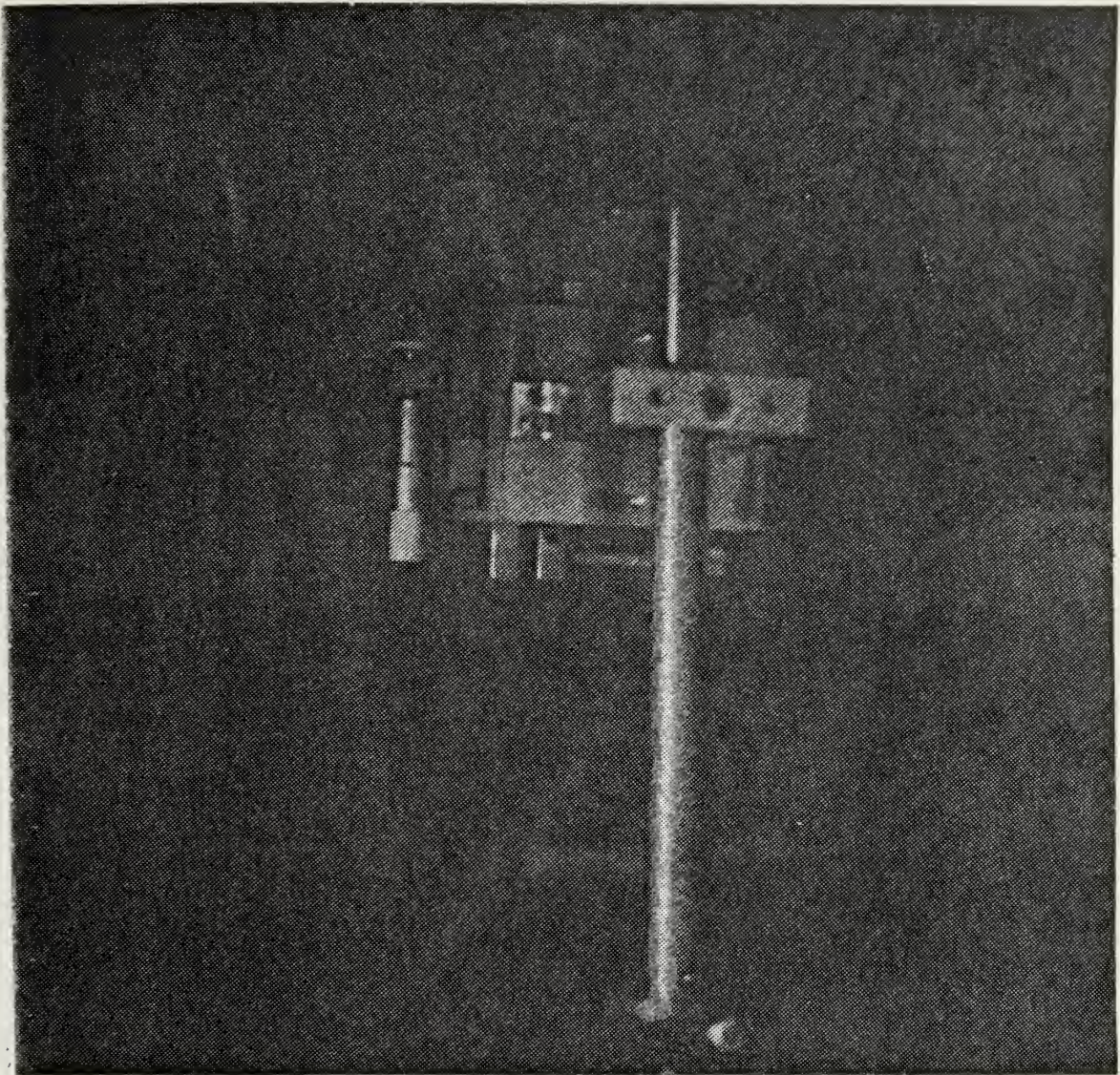




Cylinder mounted in wind tunnel and LDV setup.

Figure 5

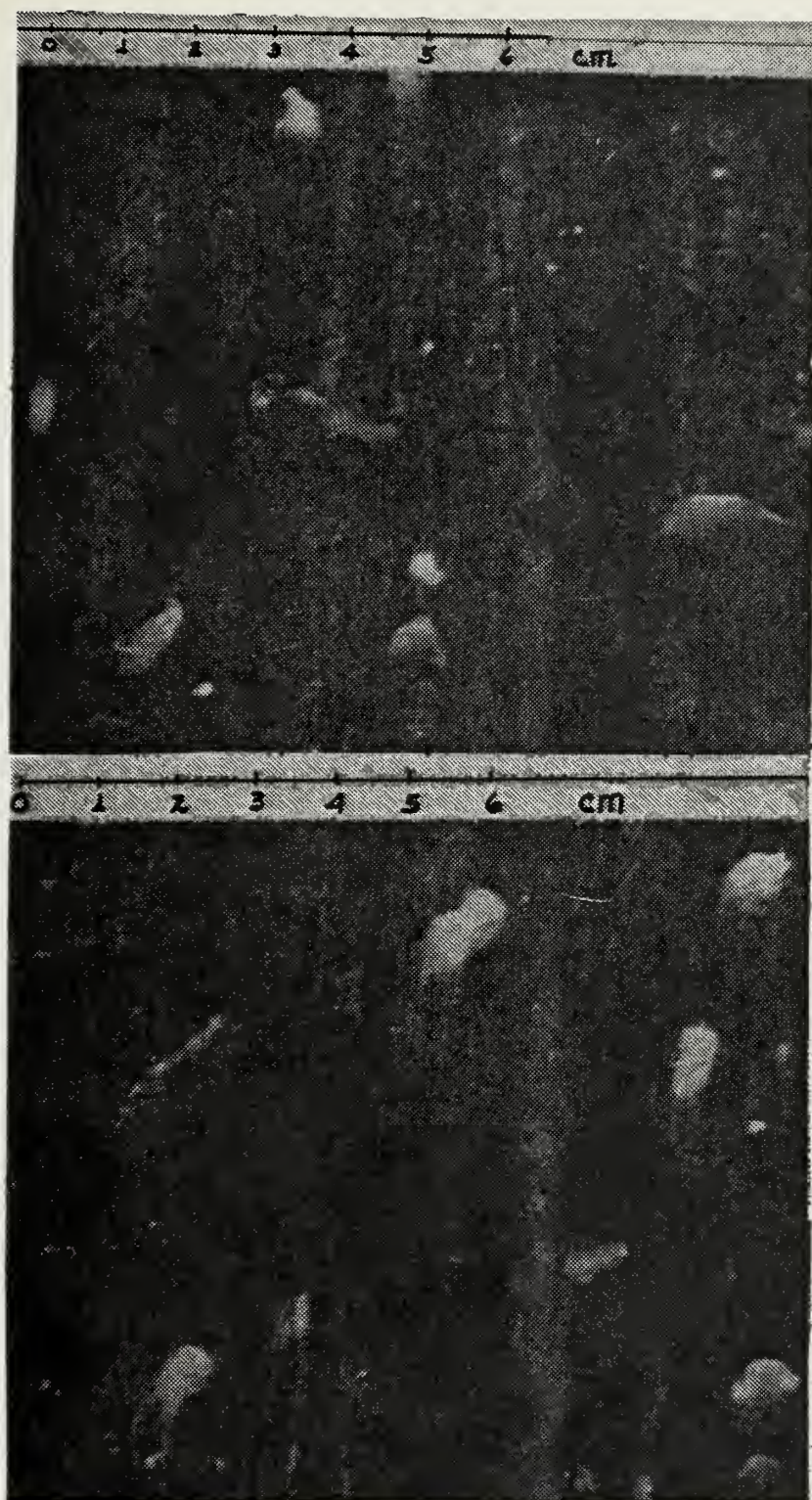




Traversing mechanism

Figure 6





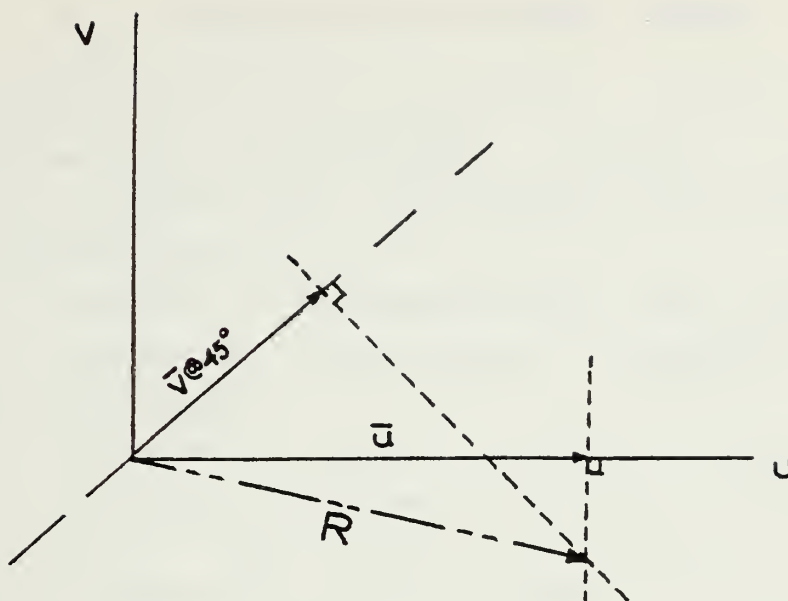
Zinc-hexachlororathane particles  
(X5000 1cm = 2.0  $\mu$ m)

Figure 7

The final velocity component measured at each node was the result of averaging three successive readings from the velocimeter processor. Each of these readings represented the average of 4096 readings which had been validated to within 1.5% of the exact five-eighths validation count criteria.

The flow in the wind tunnel was stabilized at five inches per second to maintain a Reynolds number of about 40, which is in the realm of creeping flow. The experimental setup was designed to measure the steady flow about the cylinder, hence the relatively low Reynolds number, and no effort was made to obtain unsteady flow measurements. Three separate runs were conducted, two over the forward half of the control volume and one over the rear half. Because the beams of the laser anemometer were approximately one-sixteenth inch in diameter, several node position measurements were excluded due to inaccessibility. The majority of these were in close proximity to the cylinder. In order to obtain both an x- and a y-velocity component of the flow at every node which was accessible, two measurements were made, but because of the very small vertical component present in most of the flow, direct vertical beam pair measurement was unsuitable. Instead, after obtaining the horizontal component for each node in a run, a second series of measurements was made with the beam pairs inclined forty-five degrees from the vertical. In this fashion the y-component was determined by the following relationship:





It can be seen here that the unknown resultant (R) has a projection onto each axis representing the orientation of the beam pairs, thus the resultant is the vector which emanates from the origin and terminates at the intersection of the perpendiculars constructed from the  $\bar{u}$  and  $\bar{v}$  (at 45 degrees) vectors.

## V. DESCRIPTION OF COMPUTER PROGRAM

The program found in the appendix has several comment cards inserted for clarification. However, a broader presentation is offered here. The program may be subdivided into four main sections:

Section 1: dimensioning and zeroing of parameters and arrays. (FLU00020 through FLU00690)

Section 2: input of node coordinates, system topology and known values of  $u$ ,  $v$ ,  $P$ , and right hand sides, and output of the same. (FLU00700 through FLU02090)

Section 3: computation of interpolation polynomials on an elemental level and arrangement into local element arrays. (FLU02100 through G000320)

Section 4: loading of the global influence matrix  $(TM)$  and solution of  $(TM)(T)=(Q)$  by Gauss-Jordan partial pivoting and back substitution, with an iterative routine incorporated until convergence is attained, and associated print out. (FLU04470 through FLU04880)

The computer routine systematically tested the solution of field variables with the previous solution until all terms in the  $T$  and  $T1$  arrays agreed within 0.001 (ESPILA). If the convergence test failed, the process was repeated from section 3.

Initially, the program was run on an IBM 360 in FORTRAN CLG mode, then an ensuing run was completed on the FORTRAN HCLG compiler and a time reduction of two-thirds was realized. The program, as given in the appendix, required approximately 375K bytes of core to compile and 675K bytes

to execute and output. Substantial space savings may be realized by utilizing banded matrix storage methods vice the method employed here, but due to time limitations this avenue was not fully explored.

The program attempts to solve simultaneously for all the field variables. However, introduction of zeros on the main diagonal of the TM influence matrix resulted in a singular matrix. Another approach was explored where the equation of continuity

$$\frac{\partial u}{\partial x} + \frac{\partial v}{\partial y} = 0$$

was replaced by

$$-\frac{1}{2}\nabla^2 P = \left[ \frac{\partial v}{\partial x} \frac{\partial u}{\partial y} - \frac{\partial u}{\partial x} \frac{\partial v}{\partial y} \right]$$

and the resulting terms were added to the TM matrix and their respective right hand sides. The only field variables affected by this form of the continuity equation were the pressure variables, and depending on whether the local corner node involved in the local pressure equation was on the boundary or interior, different right hand sides had to be evaluated. This is the purpose of steps FLU04460 through GO00320. The simultaneous solution technique for all field variables applied to this new set of equations did not converge.

A third, unimplemented technique may be considered. Given the original matrix equations:

$$(1) \quad K_1 U + 0 + K_2 P = R_1$$

$$(2) \quad 0 + K_1 V + K_3 P = R_2$$

$$(3) \quad K_2 U + K_3 V + 0 = 0$$

Solution for u and v will result in

$$(1) \quad U = -K_1^{-1} K_2 P + K_1^{-1} R_1$$

$$(2) \quad V = -K_1^{-1} K_3 P + K_1^{-1} R_2$$

and multiplication by  $K_2$  and  $K_3$  yields

$$K_2 U = -K_2 K_1^{-1} K_3 P + K_2 K_1^{-1} R_1$$

$$K_3 V = -K_3 K_1^{-1} K_3 P + K_3 K_1^{-1} R_2$$

Summation of these equations allows substitution for the third matrix equation:

$$\left[ K_2 K_1^{-1} K_3 + K_3 K_1^{-1} K_3 \right] P = K_2 K_1^{-1} R_1 + K_3 K_1^{-1} R_2$$

The matrix operating on  $P$  may be calculated on an algebraic level and entered, in terms of  $a_i$ ,  $b_i$  and  $c_i$ , into the program in order to solve for the pressures at every corner node. The calculated  $P$ 's then would be entered into the field variable array and the partial pivoting routine, which involves only those terms where the field variable is not specified, would operate primarily on the first two matrix equations. In previous computer trials where all corner node pressures were specified, although not known to be correct, calculations were properly performed. This method would allow the actual pressures present in the control surface to be entered into the computer routine for further calculation of the velocity components.

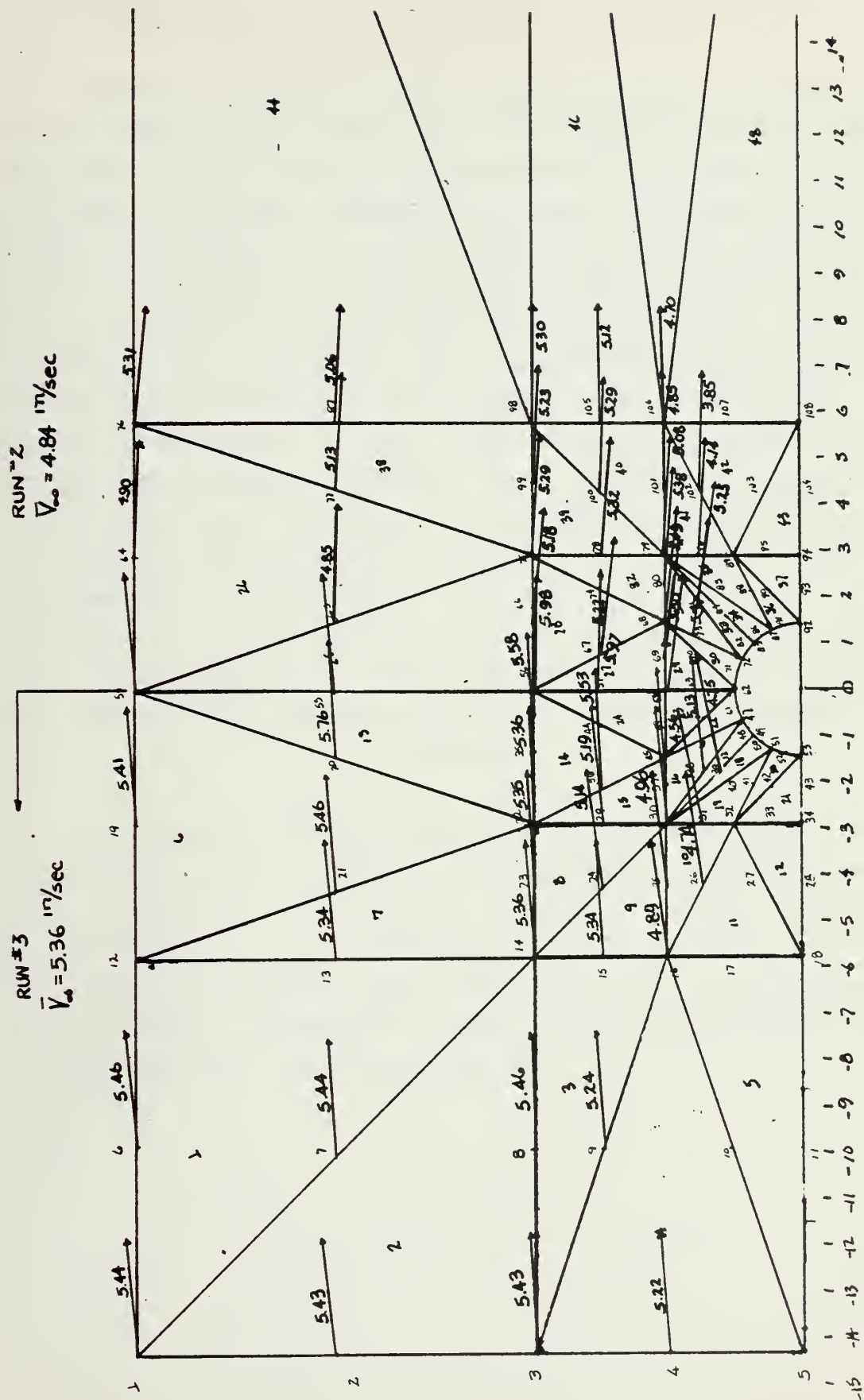
## VI. ANALYSIS OF RESULTS

No computer routine output was obtained for comparison of results, due to the inability of the program to converge. As such, comparison of the two methods cannot be offered here. The non-convergence of the program was investigated from several aspects: validity of the non-linear terms, correctness of the loading of the TM matrix on both the elemental and global levels, correctness of input, performance of the partial pivoting subroutines and the iteration scheme; all without success. In test cases the program initially solved for the unknowns within magnitude accuracy for a majority of terms. However, successive iterations resulted in oscillating solutions, even after twenty iterations. Convergence was expected after ten to fifteen iterations without under- or overrelaxation factors incorporated into the iteration scheme. After the new formulation of the continuity equation was incorporated into the computer routine, the program execution again resulted in a singular matrix when only the left and right hand and upper control surface boundaries had their respective pressures specified. Underflow occurred in the execution of the subroutine SOLVE at step SOL00260. Subsequent investigation revealed that the 178<sup>th</sup> and 179<sup>th</sup> rows of the reduced matrix equations were the cause of the underflow.

The data which were taken for runs number two and three are displayed in the appendix and are plotted on the finite element grid in Figure 8. Without the analytical results to compare the measured data only a qualitative statement may be made pertaining to the LDV output. It is readily seen that the trend of flow directions around the cylinder appears to be correct. By and large, the flow in close proximity to the cylinder was accelerated over the tcp and decelerated near the stagnation points. It is pointed out

here that the plot is a composite of two different trials, and as such, different free stream velocities were present for each run. In Figure 8 the vector representing the flow at a node was plotted and the magnitude of the vector in inches per second was displayed above the vector or by the node from which the velocity vector emanated.







## A. ERROR ANALYSIS

Re-positioning of the cylinder to its base location was accomplished with relatively low position error. Prior to each run the cylinder was aligned using the beam pairs as reference. In the horizontal mode, the beam pairs would strike the leading and trailing portions of the cylinder and reflect to positions horizontally opposed on the far side of the wind tunnel when correctly zeroed vertically. The same procedure was repeated for the vertical beam pair except position was checked by the upper beam reflecting to a vertical position on the far wall and the lower beam (at reduced intensity) striking the cylinder support on centerline. This procedure was repeated several times and the maximum deviation between any aligned positions was 0.2 millimeters horizontally or vertically. Thus, it was determined that the maximum positioning error inherent in the system would be the ratio of the smallest coordinate of any node measured and the aforementioned 0.2 millimeters or

$$0.2/3.75=0.5\%$$

Freestream velocity measurements were likewise tested for fluctuations. Typical measurement variations ranged from 0.129 to 0.142 (run number three; freestream measurements) in the horizontal mode and 0.0947 to 0.100 in the forty-five degree mode (velocities in meters/seconds). These figures represent a total of 10% variation which may be considered as  $\pm 5\%$  from the mean.

## VII. CONCLUSION

The experiment, as described, required approximately two to four hours for each run. aside from the initial alignment of the components and the cylinder, this was perhaps the greatest drawback of the system. Next, the exclusion of regions in close proximity to the cylinder from measurement was deemed to be a major factor in the small amount of data actually taken. The latter may be improved with a different experimental arrangement; particularly, the plexiglass section directly prefacing the optics transducer should be completely removed, thus allowing all angles of beam pair inclination, and in turn availing more locations to measurement. Another improvement which could be implemented would be unitization of the laser, transducer and photomultiplier tube arrangement. This would decrease the LDV's sensitivity to vibration and provide a more accurate optical axis alignment. The aforementioned improvements would still not decrease the time required for data collection, but the introduction of a two component system [Ref.4] would allow simultaneous measurement using orthogonal beam pairs. Furthermore, this type of system would not concern itself with the errors introduced in beam pair re-alignments performed with the single beam pair LDV.

The reproducibility of the experiment was judged to be good with the exception of exact duplication of the wind tunnel velocity between successive trials. This, of course, is primarily a function of the controllability of the tunnel motor and propellor assembly. It is estimated that with adequate facilities for incorporation of some of the aforementioned improvements, more accurate data may be obtained. The LDV displays great potential as a means of measuring a wide variety of dynamic fluid regimes accurately and without introduction of disturbance to the flow itself.

APPENDIX A

LDV DATA

RUN #2

Node	U(cm/sec)	$V_{\theta 45^\circ}$ (cm/sec)	R(in/sec)	$\angle^\circ$
64	12.43	8.43	4.90	-2.3
65	12.33	8.49	4.85	-1.5
66	13.10	8.33	5.18	-5.8
67	13.17	8.25	5.22	-6.5
68	13.87	8.72	5.49	-6.3
69	13.87	8.56	5.50	-7.2
73	14.03	8.58	5.57	-7.7
75	13.40	8.83	5.29	-3.9
76	13.43	8.62	5.31	-5.3
77	13.00	8.62	5.13	-3.6
78	13.47	8.87	5.32	-4.5
79	12.87	8.58	5.08	-3.3
80	13.63	8.91	5.38	-4.3
81	13.20	8.02	5.25	-8.0
96	10.50	6.94	4.14	-3.7
97	12.83	8.64	5.06	-2.7
98	13.47	9.54	5.30	0.1
99	13.27	8.92	5.23	-2.8
100	13.43	9.25	5.29	-1.5
101	12.33	8.83	4.85	0.7
102	9.77	6.69	3.85	-1.8
105	13.03	9.32	5.12	0.8
106	11.93	8.68	4.70	1.7

RUN #3

Node	U(cm/sec)	V@45°(cm/sec)	R(in/sec)	°
1	13.73	10.77	5.44	6.23
2	13.70	10.43	5.43	6.25
3	13.77	10.33	5.43	3.49
4	13.23	10.03	5.22	4.11
6	13.77	10.93	5.46	7.00
7	13.80	10.40	5.44	3.77
8	13.87	10.17	5.46	2.11
9	13.27	10.08	5.24	4.27
13	13.50	10.47	5.34	5.54
14	13.57	10.40	5.36	4.80
15	13.53	10.20	5.34	3.76
16	12.30	9.93	4.89	8.05
19	13.70	10.43	5.41	4.38
20	14.60	10.87	5.76	3.02
21	13.83	10.57	5.46	4.63
22	13.60	10.06	5.36	2.65
23	13.57	10.23	5.35	3.79
24	12.93	10.40	5.14	7.84
25	12.50	9.92	4.96	7.00
26	11.90	9.64	4.74	8.27
29	13.13	10.16	5.19	5.40
30	12.57	9.80	4.98	5.86
31	11.30	9.76	4.56	12.50
35	14.17	10.47	5.58	2.60
36	14.03	10.43	5.53	4.36
37	13.23	10.07	5.22	4.36
38	12.97	10.09	5.13	5.72
39	11.83	10.03	4.75	11.24
54	14.03	10.87	5.55	5.58
55	14.17	11.03	5.61	5.76
56	15.20	10.57	5.98	-0.90
57	15.17	10.47	5.97	-1.36
58	16.27	10.00	6.46	-7.46
59	14.37	10.20	5.66	0.20





```

C      READ IN NUMBER OF NODES AND ELEMENTS AND NO. CORNER NODES
C      READ(NREAD,1005)NN,NE,NNCN
C
C      INITIALIZE ALL PARAMETERS

```

```

      MM=NN+NN+NNCN

```

```

      DC 50 I=1,120

```

```

      XC(I)=0.

```

```

      YC(I)=0.

```

```

      NVS(I)=0

```

```

      NCP(I)=0

```

```

      NPS(I)=0

```

```

      NCS(I)=0

```

```

      50 CONTINUE

```

```

      DO 51 I=1,MM

```

```

      NVIS(I)=0

```

```

      NQIS(I)=0

```

```

      T(I)=0.

```

```

      Q(I)=0.

```

```

      Z(I)=0.

```

```

      C(I)=0.

```

```

      DO 51 J=1,MM

```

```

      B(I,J)=0.

```

```

      51 CONTINUE

```

```

      DO 53 I=1,15

```

```

      N(I)=0

```

```

      DO 53 J=1,15

```

```

      TM$(I,J)=0.

```

```

      53 CONTINUE

```

```

      DO 54 I=1,6

```

```

      RP$(I)=0.

```

```

      ZP$(I)=0.

```

```

      U(I)=0.0

```

```

      V(I)=0.0

```

```

      DO 54 K=1,6

```

```

      QZ1(I,K)=0.0

```

```

      QZB(I)=0.0

```

```

      QZC(I)=0.0

```

```

      QZ2(I,K)=0.0

```

```

      QZ3(I,K)=0.0

```

```

      54 CONTINUE

```

```

      DO 55 I=1,3

```

```

      XC$(I)=0.

```

```

      YC$(I)=0.

```

```

      NT(I)=0

```

```

      55 CONTINUE

```

```

FLU00390
FLU00400
FLU00410
FLU00420
FLU00430
FLU00440

FIX00020
FIX00030
FIX00040
FIX00050
FIX00070
FIX00080
FIX00200
FIX00090
FIX00100
FIX00060
FIX00210
FIX00110
FIX00120
FIX00130
FIX00140
FIX00150
FIX00160
FIX00170
FIX00180
FIX00230
FIX00240
FIX00250
FIX00260
FIX00270

FIX00290
FIX00300

```

```

FIX00310
FIX00320
FIX00330
FIX00340

FIX00350

```



```

DO 56 I=1,4
  NLCY(I)=0.0
  NRCY(I)=0.0
56 CONTINUE
C READ NODE NUMBERS AND COORDINATES
C
DO 100 J=1,NN
  READ(NREAD,1006)WORD,I,XC(I),YC(I)
  IF (WORD.EQ.STOP) GO TO 101
  NCN(J)=I
100 CONTINUE
101 NNCN=J-1
C
C THE ARRAY NCP(J) GENERATES THE GLOBAL PRESSURE INDICES (P1,P2.)
C THUS PRESSURE NODES ARE LABELED AS CORNER NODES ARE INPUTED
C WHEN ONE INPUTS A GLOBAL CORNER NODE FOR J
C
DO 107 J=1,NNCN
  NCP(NCN(J)) =J+NN+NN
107 CONTINUE
C
C SYSTEM TOPOLOGY( ELEMENT NO. AND NODE NUMBERS IN
C COUNTER-CLOCKWISE FASHION STARTING AT ANY CORNER NODE
C ALWAYS COUNT FROM UPPER LEFT HAND CORNER
C
DO 105 I=1,NE
  READ(NREAD,1010)J,NODE(J,1),NODE(J,2),NODE(J,3),
  1 NODE(J,4),NODE(J,5),NODE(J,6)
105 CONTINUE
  MAXDIF=0
  DO 108 I=1,NE
    DO 108 J=1,6
      DO 108 K=1,6
        LL=IABS(NODE(I,J)-NODE(I,K))
        IF(LL.GT.MAXDIF) MAXDIF=LL
      IBAND=2*(MAXDIF+1)
      NEQ=2*NN+NNCN
108 CONTINUE
107 WRITE(NWRITE,1017)IBAND,NEQ
1017 FORMAT(5X,'IBAND=',I3,'/',5X,'NEQ =',I3,'/')
C READ NODES WHERE BOTH U AND V VELOCITY IS SPECIFIED
C
DO 110 I=1,MM
  READ(NREAD,1006)WORD,NVELS,VELU,VELV
  IF(WORD.EQ.STOP) GO TO 111
  NVS(I)=NVELS
  T(NVS(I))=VELU
  T(NVS(I)+1)=VELV

```

FLU00690  
 FLU00700  
 FLU00710  
 FLU00720  
 FLU00730  
 FLU00740  
 FLU00750  
 FLU00760  
 FLU00770  
 FLU00780  
 FLU00790  
 FLU00800  
 FLU00810  
 FLU00820  
 FLU00830  
 FLU00840  
 FLU00850  
 FLU00860  
 FLU00870  
 FLU00880  
 FLU00890  
 FLU00900  
 FLU00910  
 FLU00920  
 FLU00930  
 FLU00940  
 FLU00950  
 FLU00960  
 FLU00970  
 FLU00980  
 FLU00990  
 FLU01000  
 FLU01010  
 FLU01020  
 FLU01030  
 FLU01040  
 FLU01050  
 FLU01060  
 FLU01070  
 FLU01080  
 FLU01090  
 FLU01100  
 FLU01110  
 FLU01120

```

110 T(NVS(I)+NN)=VELV
    CONTINUE
C COUNT NODES HAVING SPECIFIED VELOCITIES
C
111 NNVELS= I-1
C
C READ QX AND QY VALUES AT INTERNAL NODES
DO 125 I=1,NN
  READ(NREAD,1006)WORD,NQXY,QXNS,QYNS
  IF(WORD.EQ.STOP) GO TO 126
  NQS(I)=NQXY
  Q(NQS(I))=QXNS*PRES
  Q(NQS(I)+NN)=QYNS*PRES
125 CONTINUE
126 NNQXY=I-1
C
C READ NODE NUMBERS AND PRESSURE WHEREE PRESSURE IS SPECIFIED
C
DO 130 I=1,NN
  READ(NREAD,1025)WORD,NP,PNP
  IF(WORD.EQ.STOP)GO TO 135
  NPS(I)=NP
  T(NCP(NPS(I)))=PNP
130 CONTINUE
C COUNT BOUNDARY NODES WHERE PRESSURE SPECIFIED
C
135 NNPS= I-1
C
C READ PRESSURE NODES WHERE Q IS SPECIFIED
C
DO 141 I=1,MM
  READ(NREAD,1025)WORD,NPQ,QNPQ
  IF(WORD.EQ.STOP)GO TO 142
  NPS(I+NNPS)=NPQ
  Q(NCP(NPS(I+NNPS)))=QNPQ
141 CONTINUE
142 NNPQ=I-1
C
C READ IN CORNER NODES WHICH ARE CONTAINED IN THE INTERIOR
C
DO 143 I=1,MM
  READ(NREAD,7654) NINT

```

FLU01130  
 FLU01140  
 FLU01150  
 FLU01160  
 FLU01170  
 FLU01180  
 FLU01190  
 FLU01200  
 FLU01210  
 FLU01220  
 FLU01230  
 FLU01240  
 FLU01250  
 FLU01260

FLU01290  
 FLU01300  
 FLU01310  
 FLU01320  
 FLU01330  
 FLU01340  
 FLU01350  
 FLU01360  
 FLU01370  
 FLU01380  
 FLU01390  
 FLU01400  
 FLU01410  
 FLU01420  
 FLU01430  
 PRE00100  
 PRE00090

PRE00110  
 PRE00130  
 PRE00010  
 PRE00020  
 PRE00030  
 PRE00040  
 PRE00050  
 PRE00070  
 PRE00080  
 QZ 00160

QZ 00140  
 QZ 00070  
 QZ 00080

```

IF (WORD.EQ.STOP) GO TO 147
NI(I)=NINT
143 CONTINUE
7654 FORMAT(6X,A4,14I4)
147 CONTINUE
C
C NCIS IS A LIST OF THE INDICES OF KNOWN QX QY
C
      DO 1140 I=1,NNQXY
        NQIS(I)=NQS(I)
        NQIS(I+NNQXY)=NQS(I)+NN
1140 CONTINUE
      DO 1142 I=1,NNPQ
        NQIS(I+2*NNQXY)=NPS(I+NNPS)+2*NN
1142 CONTINUE
C
C NVIS IS A LIST OF INDICIES OF KNOWN VELOCITIES AND PRESSURES
C
      DO 1150 I=1,NNVELS
        NVIS(I)=NVS(I)
        NVIS(I+NNVELS)=NVS(I)+NN
1150 CONTINUE
      DO 1160 J=1,NNPS
        NVIS(2*NNVELS+J)=NCP(NPS(J))
1160 CONTINUE
C
C NTOTQ TOTAL NUMBER OF KNOWN QX AND QY
C
      NTOTQ=2*NNQXY +NNPQ
      NTOTVP=2*NNVELS+NNPS
C
C PRINT ALL INPUT DATA
C
      WRITE(NWRITE,1035)NN,NE,NNCN
      WRITE(NWRITE,1040)
      DO 150 I=1,NNCN
        WRITE(NWRITE,1045)NCN(I),XC(NCN(I)),YC(NCN(I))
        CONTINUE
150 WRITE(NWRITE,1050)
      DO 155 I=1,NE
        WRITE(NWRITE,1055)I,NODE(I,1),NODE(I,2),NODE(I,3),
          1 NODE(I,4),NODE(I,5),NODE(I,6)
155 CONTINUE
      WRITE(NWRITE,1060)
      DO 160 I=1,NNVELS
        WRITE(NWRITE,1065)I,NVS(I),T(NVS(I)),T(NVS(I)+NN)
160 CONTINUE
      WRITE(NWRITE,1070)

```

QZ 00100  
8Z 00 10

FLU01440  
FLU01450  
FLU01460  
FLU01470  
FLU01480  
FLU01490  
FLU01500

FLU01510  
FLU01530  
FLU01540  
FLU01550  
FLU01560  
FLU01570  
FLU01580  
FLU01590  
FLU01600  
FLU01610  
FLU01620  
FLU01630  
FLU01640

FLU01710  
FLU01720  
FLU01730  
FLU01740  
FLU01750  
FLU01760  
FLU01770  
FLU01780  
FLU01790  
FLU01800  
FLU01810  
FLU01820  
FLU01830  
FLU01840  
FLU01850  
FLU01860  
FLU01870  
FLU01880

```

DO 165 I=1,NNQXY
WRITE(NWRITE,1065)I,NQS(I),Q(NQS(I)),Q(NQS(I)+NN)
165 CONTINUE
IF(NNPQ.EQ.0)GO TO 163
WRITE(NWRITE,1071)
DO 163 I=1,NNPQ
WRITE(NWRITE,1072)I,NPS(I+NNPS),Q(NCP(NPS(I+NNPS)))
163 CONTINUE
WRITE(NWRITE,1080)
DO 170 I=1,NNPS
WRITE(NWRITE,1085)I,NPS(I),T(NCP(NPS(I)))
170 CONTINUE
177 CONTINUE
DO 179 I=1,MM
RHS(I)=0.0
DO 179 J=1,MM
TM(I,J)=0.0
CONTINUE
175 CONTINUE
END OF INPUT AND VERIFICATION ROUTINE
CCCC
DO 300 K=1,NE
N1=NODE(K,1)
N2=NODE(K,2)
N3=NODE(K,3)
N4=NODE(K,4)
N5=NODE(K,5)
N6=NODE(K,6)
N7 = NODE(K,1)+NN
N8 = NODE(K,2)+NN
N9 = NODE(K,3)+NN
N10=NODE(K,4)+NN
N11=NODE(K,5)+NN
N12=NODE(K,6)+NN
N13=NCP(NODE(K,1))
N14=NCP(NODE(K,3))
N15=NCP(NODE(K,5))
XC$(1)=XC(NODE(K,1))
XC$(2)=XC(NODE(K,3))
XC$(3)=XC(NODE(K,5))
YC$(1)=YC(NODE(K,1))
YC$(2)=YC(NODE(K,3))
YC$(3)=YC(NODE(K,5))
A=.0229248
AA=1.
A1=XC$(2)*YC$(3)-XC$(3)*YC$(2)
A2=XC$(3)*YC$(1)-XC$(1)*YC$(3)
A3=XC$(1)*YC$(2)-XC$(2)*YC$(1)

```

```

B1=YC$(2)-YC$(3)
B2=YC$(3)-YC$(1)
B3=YC$(1)-YC$(2)
C1=XC$(3)-XC$(2)
C2=XC$(2)-XC$(1)
C3=XC$(1)-XC$(3)
DEL=ABS(0.5*(YC$(1)-YC$(2)))+(YC$(3)-YC$(1))+XC$(1)
1 3)*(YC$(1)-YC$(2)))*AA
CONST=(1.*A/(3.*DEL))*AA
D1=-B1/6.
D2=-B2/6.
D3=-B3/6.
E1=-C1/6.
E2=-C2/6.
E3=-C3/6.
F1=B1/2520.
F2=B2/2520.
F3=B3/2520.
G1=C1/2520.
G2=C2/2520.
G3=C3/2520.
U1=T1(N1)
U2=T1(N2)
U3=T1(N3)
U4=T1(N4)
U5=T1(N5)
U6=T1(N6)
V1=T1(N7)
V2=T1(N8)
V3=T1(N9)
V4=T1(N10)
V5=T1(N11)
V6=T1(N12)
TM$(1,1)=.75*(B1*B1+C1*C1)*CONST
TM$(1,2)=(B1*B2+C1*C2)*CONST
TM$(1,3)=-TM$(1,2)*.25
TM$(1,4)=0.
TM$(1,6)=(B1*B3+C1*C3)*CONST
TM$(1,5)=-TM$(1,6)*.25
TM$(3,3)=.75*(B2*B2+C2*C2)*CONST
TM$(3,4)=(B2*B3+C2*C3)*CONST
TM$(3,5)=-TM$(3,4)*.25
TM$(1,2)=TM$(1,2)
TM$(2,1)=TM$(1,2)
TM$(2,3)=TM$(1,2)
TM$(2,2)=8./3.*(TM$(1,1)+TM$(3,3))+2.*TM$(1,2)
TM$(2,4)=2.*TM$(1,6)+TM$(3,4)+TM$(1,2)+4./3.*TM$(3,3)
TM$(2,5)=0.
TM$(2,6)=TM$(1,6)+2.*TM$(3,4)+TM$(1,2)+4./3.*TM$(1,1)

```

```

FLU02380
FLU02390
FLU02400
FLU02410
FLU02420
FLU02430
FLU02440
FLU02450
FLU02460
FLU02470
FLU02480
FLU02490
FLU02500
FLU02510
FLU02520
FI X00010
FI X00020
FI X00030
FI X00040
FI X00050
FI X00060
FI X00080
FI X00090
FI X00100
FI X00110
FI X00120
FI X00130
FI X00140
FI X00150
FI X00160
FI X00170
FI X00180
FI X00190
FLU02590
FLU02600
FLU02610
FLU02620
FLU02630
FLU02640
FLU02650
FLU02660
FLU02670
FLU02680
FLU02690
FLU02700
FLU02710
FLU02720
FLU02730

```



```

TM$(3,1)=TM$(1,3)
TM$(3,2)=TM$(2,3)
TM$(3,6)=0.
      TM$(5,5)=.75 *(B3*B3+C3*C3)*CONST
TM$(4,1)=TM$(1,4)
TM$(4,2)=TM$(2,4)
TM$(4,3)=TM$(3,4)
TM$(4,4)=8./3.*(TM$(3,3)+TM$(5,5))+2.*TM$(3,4)
TM$(4,5)=TM$(3,4)
TM$(4,6)=TM$(1,6)+TM$(3,4)+2.*TM$(1,2)+4./3.*TM$(5,5)
TM$(6,3)=TM$(3,6)
TM$(5,1)=TM$(1,5)
TM$(5,2)=TM$(2,5)
TM$(5,3)=TM$(3,5)
TM$(5,4)=TM$(4,5)
TM$(5,6)=TM$(1,6)
TM$(6,1)=TM$(1,6)
TM$(6,2)=TM$(2,6)
TM$(6,4)=TM$(4,6)
TM$(6,5)=TM$(5,6)
TM$(6,6)=8./3.*(TM$(5,5)+TM$(1,1))+2.*TM$(1,6)
      IF(NCASE.NE.1)GO TO 3000

```

```

FLU02740
FLU02750
FLU02760
FLU02770
FLU02780
FLU02790
FLU02800
FLU02810
FLU02820
FLU02830
FLU02840
FLU02850
FLU02860
FLU02870
FLU02880
FLU02890
FLU02900
FLU02910
FLU02920
FLU02930
FLU02940
FLU02950

```

CCCC

# BEGIN INPUT OF NON-LINEAR TERMS

```

1 TM$(1,1)=TM$(1,1)-
  (F1*(78.*U1+48.*U2+(-9.*U3)+12.*U4+(-9.*U5)+48.*U6))
1 TM$(1,2)=TM$(1,2)-
  (F2*(120.*U1+48.*U2-16.*U3-16.*U4-16.*U5+48.*U6))-
2 (F1*(24.*U1-32.*U2-16.*U3-48.*U4+4.*U5-16.*U6))
1 TM$(1,3)=TM$(1,3)-
  (F2*(-18.*U1-32.*U2-9.*U3-20.*U4+11.*U5-16.*U6))
1 TM$(1,4)=TM$(1,4)-
  (F3*(24.*U1-32.*U2-16.*U3-48.*U4+4.*U5-16.*U6))-
2 (F2*(24.*U1-16.*U2+4.*U3-48.*U4-16.*U5-32.*U6))
1 TM$(1,5)=TM$(1,5)-
  (F3*(-18.*U1-16.*U2+11.*U3-20.*U4-9.*U5-32.*U6))
1 TM$(1,6)=TM$(1,6)-
  (F3*(120.*U1+48.*U2-16.*U3-16.*U4-16.*U5+48.*U6))-
2 (F1*(24.*U1-16.*U2+4.*U3-48.*U4-16.*U5-32.*U6))
1 TM$(2,1)=TM$(2,1)-
  (F1*(48.*U1+160.*U2-32.*U3+16.*U4-20.*U5+80.*U6))
1 TM$(2,2)=TM$(2,2)-
  (F2*(48.*U1+384.*U2-32.*U3+128.*U4-48.*U5+192.*U6))-
2 (F1*(-32.*U1+384.*U2+48.*U3+192.*U4-48.*U5+128.*U6))
1 TM$(2,3)=TM$(2,3)-

```

```

FIX00190
FIX00200
FIX00210
FIX00220
FIX00230
FIX00240
FIX00250
FIX00260
FIX00270
FIX00280
FIX00290
FIX00300
FIX00310
FIX00320
FIX00330
FIX00340
FIX00350
FIX00370
FIX00380
FIX00390
FIX00400

```



1 (F2\*(-32.\*U1+160.\*U2+48.\*U3+80.\*U4-20.\*U5+16.\*U6))  
TM\$(2,4)=TM\$(2,4)  
1 (F3\*(-32.\*U1+384.\*U2+48.\*U3+192.\*U4-48.\*U5+128.\*U6))-  
2 (F2\*(-16.\*U1+128.\*U2-16.\*U3+128.\*U4-16.\*U5+128.\*U6))  
TM\$(2,5)=TM\$(2,5)  
1 (F3\*(-16.\*U1-96.\*U2-16.\*U3+16.\*U4+12.\*U5+16.\*U6))  
TM\$(2,6)=TM\$(2,6)  
1 (F3\*(48.\*U1+384.\*U2-32.\*U3+128.\*U4-48.\*U5+192.\*U6))-  
2 (F1\*(-16.\*U1+128.\*U2-16.\*U3+128.\*U4-16.\*U5+128.\*U6))  
TM\$(3,1)=TM\$(3,1)  
1 (F1\*(-9.\*U1-32.\*U2-18.\*U3-16.\*U4+11.\*U5-20.\*U6))  
TM\$(3,2)=TM\$(3,2)  
1 (F2\*(-16.\*U1-32.\*U2+24.\*U3-16.\*U4+4.\*U5-48.\*U6))-  
2 (F1\*(-16.\*U1+48.\*U2+120.\*U3+48.\*U4-16.\*U5-16.\*U6))  
TM\$(3,3)=TM\$(3,3)  
1 (F2\*(-9.\*U1+48.\*U2+78.\*U3+48.\*U4-9.\*U5+12.\*U6))  
TM\$(3,4)=TM\$(3,4)  
1 (F3\*(-16.\*U1+48.\*U2+120.\*U3+48.\*U4-16.\*U5-16.\*U6))-  
2 (F2\*(4.\*U1-16.\*U2+24.\*U3-32.\*U4-16.\*U5-48.\*U6))  
TM\$(3,5)=TM\$(3,5)  
1 (F3\*(11.\*U1-16.\*U2-18.\*U3-32.\*U4-9.\*U5-20.\*U6))  
TM\$(3,6)=TM\$(3,6)  
1 (F3\*(-16.\*U1-32.\*U2+24.\*U3-16.\*U4+4.\*U5-48.\*U6))-  
2 (F1\*(4.\*U1-16.\*U2+24.\*U3-32.\*U4-16.\*U5-48.\*U6))  
TM\$(4,1)=TM\$(4,1)  
1 (F1\*(12.\*U1+16.\*U2-16.\*U3-96.\*U4-16.\*U5+16.\*U6))  
TM\$(4,2)=TM\$(4,2)  
1 (F2\*(-16.\*U1+128.\*U2-16.\*U3+128.\*U4-16.\*U5+128.\*U6))-  
2 (F1\*(-48.\*U1+192.\*U2+48.\*U3+384.\*U4-32.\*U5+128.\*U6))  
TM\$(4,3)=TM\$(4,3)  
1 (F2\*(-20.\*U1+80.\*U2+48.\*U3+160.\*U4-32.\*U5+16.\*U6))  
TM\$(4,4)=TM\$(4,4)  
1 (F3\*(-48.\*U1+192.\*U2+48.\*U3+384.\*U4-32.\*U5+128.\*U6))-  
2 (F2\*(-48.\*U1+128.\*U2-32.\*U3+384.\*U4+48.\*U5+192.\*U6))  
TM\$(4,5)=TM\$(4,5)  
1 (F3\*(-20.\*U1+16.\*U2-32.\*U3+160.\*U4+48.\*U5+80.\*U6))  
TM\$(4,6)=TM\$(4,6)  
1 (F3\*(-16.\*U1+128.\*U2-16.\*U3+128.\*U4-16.\*U5+128.\*U6))-  
2 (F1\*(-48.\*U1+128.\*U2-32.\*U3+384.\*U4+48.\*U5+192.\*U6))  
TM\$(5,1)=TM\$(5,1)  
1 (F1\*(-9.\*U1-20.\*U2+11.\*U3-16.\*U4-18.\*U5-32.\*U6))  
TM\$(5,2)=TM\$(5,2)  
1 (F2\*(-16.\*U1-48.\*U2+4.\*U3-16.\*U4+24.\*U5-32.\*U6))-  
2 (F1\*(4.\*U1-48.\*U2-16.\*U3-32.\*U4+24.\*U5-16.\*U6))  
TM\$(5,3)=TM\$(5,3)  
1 (F2\*(11.\*U1-20.\*U2-9.\*U3-32.\*U4-18.\*U5-16.\*U6))  
TM\$(5,4)=TM\$(5,4)  
1 (F3\*(4.\*U1-48.\*U2-16.\*U3-32.\*U4+24.\*U5-16.\*U6))-

FI X00410  
FI X00420  
FI X00430  
FI X00440  
FI X00450  
FI X00460  
FI X00470  
FI X00480  
FI X00490  
FI X00500  
FI X00510  
FI X00520  
FI X00530  
FI X00540  
FI X00550  
FI X00560  
FI X00570  
FI X00580  
FI X00590  
FI X00600  
FI X00610  
FI X00620  
FI X00630  
FI X00640  
FI X00650  
FI X00660  
FI X00670  
FI X00690  
FI X00700  
FI X00710  
FI X00720  
FI X00730  
FI X00740  
FI X00750  
FI X00760  
FI X00770  
FI X00780  
FI X00790  
FI X00800  
FI X00810  
FI X00820  
FI X00830  
FI X00840  
FI X00850  
FI X00860  
FI X00870  
FI X00880

2 (F2\*(-16.\*U1-16.\*U2-16.\*U3+48.\*U4+120.\*U5+48.\*U6))  
 TM\$(5,5)=TM\$(5,5)-  
 1 (F3\*(-9.\*U1+12.\*U2-9.\*U3+48.\*U4+78.\*U5+48.\*U6))  
 TM\$(5,6)=TM\$(5,6)-  
 1 (F3\*(-16.\*U1-48.\*U2+4.\*U3-16.\*U4+24.\*U5-32.\*U6))-  
 2 (F1\*(-16.\*U1-16.\*U2-16.\*U3+48.\*U4+120.\*U5+48.\*U6))  
 TM\$(6,1)=TM\$(6,1)-  
 1 (F1\*(48.\*U1+80.\*U2-20.\*U3+16.\*U4-32.\*U5+160.\*U6))  
 TM\$(6,2)=TM\$(6,2)-  
 1 (F2\*(48.\*U1+192.\*U2-48.\*U3+128.\*U4-32.\*U5+384.\*U6))-  
 2 (F1\*(-16.\*U1+128.\*U2-16.\*U3+128.\*U4-16.\*U5+128.\*U6))  
 TM\$(6,3)=TM\$(6,3)-  
 1 (F2\*(-16.\*U1+16.\*U2+12.\*U3+16.\*U4-16.\*U5-96.\*U6))  
 TM\$(6,4)=TM\$(6,4)-  
 1 (F2\*(-16.\*U1+128.\*U2-16.\*U3+128.\*U4-16.\*U5+128.\*U6))-  
 2 (F3\*(-32.\*U1+128.\*U2-48.\*U3+192.\*U4+48.\*U5+384.\*U6))  
 TM\$(6,5)=TM\$(6,5)-  
 1 (F3\*(-32.\*U1+16.\*U2-20.\*U3+80.\*U4+48.\*U5+160.\*U6))  
 TM\$(6,6)=TM\$(6,6)-  
 1 (F3\*(48.\*U1+192.\*U2-48.\*U3+128.\*U4-32.\*U5+384.\*U6))-  
 2 (F1\*(-32.\*U1+128.\*U2-48.\*U3+192.\*U4+48.\*U5+384.\*U6))  
 TM\$(1,1)=TM\$(1,1)-  
 1 (G1\*(78.\*V1+48.\*V2+(-9.\*V3)+12.\*V4+(-9.\*V5)+48.\*V6))  
 TM\$(1,2)=TM\$(1,2)-  
 1 (G2\*(120.\*V1+48.\*V2-16.\*V3-16.\*V4-16.\*V5+48.\*V6))-  
 2 (G1\*(24.\*V1-32.\*V2-16.\*V3-48.\*V4+4.\*V5-16.\*V6))  
 TM\$(1,3)=TM\$(1,3)-  
 1 (G2\*(-18.\*V1-32.\*V2-9.\*V3-20.\*V4+11.\*V5-16.\*V6))  
 TM\$(1,4)=TM\$(1,4)-  
 1 (G3\*(24.\*V1-32.\*V2-16.\*V3-48.\*V4+4.\*V5-16.\*V6))-  
 2 (G2\*(24.\*V1-16.\*V2+4.\*V3-48.\*V4-16.\*V5-32.\*V6))  
 TM\$(1,5)=TM\$(1,5)-  
 1 (G3\*(-18.\*V1-16.\*V2+11.\*V3-20.\*V4-9.\*V5-32.\*V6))  
 TM\$(1,6)=TM\$(1,6)-  
 1 (G3\*(120.\*V1+48.\*V2-16.\*V3-16.\*V4-16.\*V5+48.\*V6))-  
 2 (G1\*(24.\*V1-16.\*V2+4.\*V3-48.\*V4-16.\*V5-32.\*V6))  
 TM\$(2,1)=TM\$(2,1)-  
 1 (G1\*(48.\*V1+160.\*V2-32.\*V3+16.\*V4-20.\*V5+80.\*V6))  
 TM\$(2,2)=TM\$(2,2)-  
 1 (G2\*(48.\*V1+384.\*V2-32.\*V3+128.\*V4-48.\*V5+192.\*V6))-  
 2 (G1\*(-32.\*V1+384.\*V2+48.\*V3+192.\*V4-48.\*V5+128.\*V6))  
 TM\$(2,3)=TM\$(2,3)-  
 1 (G2\*(-32.\*V1+160.\*V2+48.\*V3+80.\*V4-20.\*V5+16.\*V6))  
 TM\$(2,4)=TM\$(2,4)-  
 1 (G3\*(-32.\*V1+384.\*V2+48.\*V3+192.\*V4-48.\*V5+128.\*V6))-

F1X00890  
 F1X00900  
 F9X00 0  
 F1X00920  
 F1X00930  
 F1X00940  
 F1X00950  
 F1X00960  
 F1X00970  
 F1X00980  
 F1X00990  
 F1X01000  
 F1X01010  
 F1X01020  
 F1X01030  
 F1X01040  
 F1X01050  
 F1X01060  
 F1X01070  
 F1X01080  
 F1X01090  
 F1X01100  
 F1X01110  
 F1X00200  
 F1X00210  
 F1X00220  
 F1X00230  
 F1X00240  
 F1X00250  
 F1X00260  
 F1X00270  
 F1X00280  
 F1X00290  
 F1X00300  
 F1X00310  
 F1X00320  
 F1X00330  
 F1X00340  
 F1X00350  
 F1X00360  
 F1X00370  
 F1X00380  
 F1X00390  
 F1X00400  
 F1X00410  
 F1X00420  
 F1X00430  
 F1X00440

2(G2\*(-16.\*V1+128.\*V2-16.\*V3+128.\*V4-16.\*V5+128.\*V6))  
 TM\$(2,5)=-TM\$(2,5)-  
 1(G3\*(-16.\*V1-96.\*V2-16.\*V3+16.\*V4+12.\*V5+16.\*V6))  
 TM\$(2,6)=-TM\$(2,6)-  
 1(G3\*(-48.\*V1+384.\*V2-32.\*V3+128.\*V4-48.\*V5+192.\*V6))-  
 2(G1\*(-16.\*V1+128.\*V2-16.\*V3+128.\*V4-16.\*V5+128.\*V6))  
 TM\$(3,1)=-TM\$(3,1)-  
 1(G1\*(-9.\*V1-32.\*V2-18.\*V3-16.\*V4+11.\*V5-20.\*V6))  
 TM\$(3,2)=-TM\$(3,2)-  
 1(G2\*(-16.\*V1-32.\*V2+24.\*V3-16.\*V4+4.\*V5-48.\*V6))-  
 2(G1\*(-16.\*V1+48.\*V2+120.\*V3+48.\*V4-16.\*V5-16.\*V6))  
 TM\$(3,3)=-TM\$(3,3)-  
 1(G2\*(-9.\*V1+48.\*V2+78.\*V3+48.\*V4-9.\*V5+12.\*V6))  
 TM\$(3,4)=-TM\$(3,4)-  
 1(G3\*(-16.\*V1+48.\*V2+120.\*V3+48.\*V4-16.\*V5-16.\*V6))-  
 2(G2\*(-4.\*V1-16.\*V2+24.\*V3-32.\*V4-16.\*V5-48.\*V6))  
 TM\$(3,5)=-TM\$(3,5)-  
 1(G3\*(-11.\*V1-16.\*V2-18.\*V3-32.\*V4-9.\*V5-20.\*V6))  
 TM\$(3,6)=-TM\$(3,6)-  
 1(G3\*(-16.\*V1-32.\*V2+24.\*V3-16.\*V4+4.\*V5-48.\*V6))-  
 2(G1\*(-4.\*V1-16.\*V2+24.\*V3-32.\*V4-16.\*V5-48.\*V6))  
 TM\$(4,1)=-TM\$(4,1)-  
 1(G1\*(-12.\*V1+16.\*V2-16.\*V3-96.\*V4-16.\*V5+16.\*V6))  
 TM\$(4,2)=-TM\$(4,2)-  
 1(G2\*(-16.\*V1+128.\*V2-16.\*V3+128.\*V4-16.\*V5+128.\*V6))-  
 2(G1\*(-48.\*V1+192.\*V2+48.\*V3+384.\*V4-32.\*V5+128.\*V6))  
 TM\$(4,3)=-TM\$(4,3)-  
 1(G2\*(-20.\*V1+80.\*V2+48.\*V3+160.\*V4-32.\*V5+16.\*V6))  
 TM\$(4,4)=-TM\$(4,4)-  
 1(G3\*(-48.\*V1+192.\*V2+48.\*V3+384.\*V4-32.\*V5+128.\*V6))-  
 2(G2\*(-48.\*V1+128.\*V2-32.\*V3+384.\*V4+48.\*V5+192.\*V6))  
 TM\$(4,5)=-TM\$(4,5)-  
 1(G3\*(-20.\*V1+16.\*V2-32.\*V3+160.\*V4+48.\*V5+80.\*V6))  
 TM\$(4,6)=-TM\$(4,6)-  
 1(G3\*(-16.\*V1+128.\*V2-16.\*V3+128.\*V4-16.\*V5+128.\*V6))-  
 2(G1\*(-48.\*V1+128.\*V2-32.\*V3+384.\*V4+48.\*V5+192.\*V6))  
 TM\$(5,1)=-TM\$(5,1)-  
 1(G1\*(-9.\*V1-20.\*V2+11.\*V3-16.\*V4-18.\*V5-32.\*V6))  
 TM\$(5,2)=-TM\$(5,2)-  
 1(G2\*(-16.\*V1-48.\*V2+4.\*V3-16.\*V4+24.\*V5-32.\*V6))-  
 2(G1\*(-4.\*V1-48.\*V2-16.\*V3-32.\*V4+24.\*V5-16.\*V6))  
 TM\$(5,3)=-TM\$(5,3)-  
 1(G2\*(-11.\*V1-20.\*V2-9.\*V3-32.\*V4-18.\*V5-16.\*V6))  
 TM\$(5,4)=-TM\$(5,4)-  
 1(G3\*(-4.\*V1-48.\*V2-16.\*V3-32.\*V4+24.\*V5-16.\*V6))-  
 2(G2\*(-16.\*V1-16.\*V2-16.\*V3+48.\*V4+120.\*V5+48.\*V6))  
 TM\$(5,5)=-TM\$(5,5)-  
 1(G3\*(-9.\*V1+12.\*V2-9.\*V3+48.\*V4+78.\*V5+48.\*V6))

F1X00450  
 F1X00460  
 F1X00470  
 F1X00480  
 F1X00490  
 F1X00500  
 F1X00510  
 F1X00520  
 F1X00530  
 F1X00540  
 F1X00550  
 F1X00560  
 F1X00570  
 F1X00580  
 F1X00590  
 F1X00600  
 F1X00610  
 F1X00620  
 F1X00630  
 F1X00640  
 F1X00650  
 F1X00660  
 F1X00670  
 F1X00680  
 F1X00690  
 F1X00700  
 F1X00710  
 F1X00720  
 F1X00730  
 F1X00740  
 F1X00750  
 F1X00760  
 F1X00770  
 F1X00780  
 F1X00790  
 F1X00800  
 F1X00810  
 F1X00820  
 F1X00830  
 F1X00840  
 F1X00850  
 F1X00860  
 F1X00870  
 F1X00880  
 F1X00890  
 F1X00900  
 F1X00910  
 F1X00920





TM\$(11,11,10)=TM\$(5,2)  
TM\$(11,11,9)=TM\$(5,3)  
TM\$(11,11,8)=TM\$(5,4)  
TM\$(11,11,7)=TM\$(5,5)  
TM\$(11,11,6)=TM\$(5,6)  
TM\$(12,12,7)=TM\$(6,1)  
TM\$(12,12,8)=TM\$(6,2)  
TM\$(12,12,9)=TM\$(6,3)  
TM\$(12,12,10)=TM\$(6,4)  
TM\$(12,12,11)=TM\$(6,5)  
TM\$(12,12,12)=TM\$(6,6)  
TM\$(13,13,1)=D1  
TM\$(14,14,1)=0.  
TM\$(15,15,1)=0.  
TM\$(16,16,1)=TM\$(15,1)  
TM\$(17,17,1)=D1+2.\*D2  
TM\$(18,18,1)=TM\$(13,2)  
TM\$(19,19,1)=2.\*D1+D2  
TM\$(20,20,1)=TM\$(14,2)  
TM\$(21,21,1)=D1+D2  
TM\$(22,22,1)=TM\$(15,2)  
TM\$(23,23,1)=0.  
TM\$(24,24,1)=TM\$(13,3)  
TM\$(25,25,1)=D2  
TM\$(26,26,1)=TM\$(14,3)  
TM\$(27,27,1)=0.  
TM\$(28,28,1)=TM\$(15,3)  
TM\$(29,29,1)=D2+D3  
TM\$(30,30,1)=TM\$(13,4)  
TM\$(31,31,1)=D2+2.\*D3  
TM\$(32,32,1)=TM\$(14,4)  
TM\$(33,33,1)=2.\*D2+D3  
TM\$(34,34,1)=TM\$(15,4)  
TM\$(35,35,1)=0.  
TM\$(36,36,1)=TM\$(13,5)  
TM\$(37,37,1)=0.  
TM\$(38,38,1)=TM\$(14,5)  
TM\$(39,39,1)=D3  
TM\$(40,40,1)=TM\$(15,5)  
TM\$(41,41,1)=D1+2.\*D3  
TM\$(42,42,1)=TM\$(13,6)  
TM\$(43,43,1)=D1+D3  
TM\$(44,44,1)=D1+D3  
TM\$(45,45,1)=2.\*D1+D3  
TM\$(46,46,1)=TM\$(15,6)

FLU03630  
FLU03640  
FLU03650  
FLU03660  
FLU03670  
FLU03680  
FLU03690  
FLU03700  
FLU03710  
FLU03720  
FLU03730  
FLU03740  
FLU03750  
FLU03760  
FLU03770  
FLU03780  
FLU03790  
FLU03800  
FLU03810  
FLU03820  
FLU03830  
FLU03840  
FLU03850  
FLU03860  
FLU03870  
FLU03880  
FLU03890  
FLU03900  
FLU03910  
FLU03920  
FLU03930  
FLU03940  
FLU03950  
FLU03960  
FLU03970  
FLU03980  
FLU03990  
FLU04000  
FLU04010  
FLU04020  
FLU04030  
FLU04040  
FLU04050  
FLU04060  
FLU04070  
FLU04080  
FLU04090  
FLU04100



FLU04110  
FLU041120  
FLU041130  
FLU041140  
FLU041150  
FLU041160  
FLU041170  
FLU041180  
FLU041190  
FLU04200  
FLU04210  
FLU04220  
FLU04230  
FLU04240  
FLU04250  
FLU04260  
FLU04270  
FLU04280  
FLU04290  
FLU04300  
FLU04310  
FLU04320  
FLU04330  
FLU04340  
FLU04350  
FLU04360  
FLU04370  
FLU04380  
FLU04390  
FLU04400  
FLU04410  
FLU04420  
FLU04430  
FLU04440  
FLU04450  
FLU04460

QZ 00170

TM\$(13,13)=EI  
TM\$(7,13)=TM\$(13,7)  
TM\$(14,17)=0  
TM\$(7,14)=TM\$(14,7)  
TM\$(15,17)=0  
TM\$(7,15)=TM\$(15,7)  
TM\$(13,18)=EI+2.\*E2  
TM\$(8,13)=TM\$(13,8)  
TM\$(8,14)=2.\*EI+E2  
TM\$(8,18)=TM\$(14,8)  
TM\$(15,8)=EI+E2  
TM\$(8,15)=TM\$(15,8)  
TM\$(13,19)=0  
TM\$(9,13)=TM\$(13,9)  
TM\$(9,14)=EI  
TM\$(9,19)=TM\$(14,9)  
TM\$(15,19)=0  
TM\$(9,15)=TM\$(15,9)  
TM\$(13,10)=EI+2.\*E3  
TM\$(10,13)=TM\$(13,10)  
TM\$(14,10)=EI+2.\*E3  
TM\$(10,15)=TM\$(14,10)  
TM\$(10,15)=TM\$(15,10)  
TM\$(13,11)=0  
TM\$(11,13)=TM\$(13,11)  
TM\$(14,11)=0  
TM\$(11,14)=TM\$(14,11)  
TM\$(15,11)=EI  
TM\$(11,15)=TM\$(15,11)  
TM\$(13,12)=EI+EI+E3  
TM\$(12,13)=TM\$(13,12)  
TM\$(14,12)=EI+E3  
TM\$(12,14)=TM\$(14,12)  
TM\$(15,12)=2.\*EI+E3  
TM\$(12,15)=TM\$(15,12)  
CONST2=1/(4.\*DEL)  
TM\$(13,13)=-.5\*(B1\*B1+C1\*C1)\*CONST2  
TM\$(13,14)=-.5\*(B1\*B2+C1\*C2)\*CONST2  
TM\$(13,15)=-.5\*(B1\*B3+C1\*C3)\*CONST2  
TM\$(14,13)=TM\$(13,14)  
TM\$(14,14)=-.5\*(B2\*B2+C2\*C2)\*CONST2  
TM\$(14,15)=-.5\*(B2\*B3+C2\*C3)\*CONST2  
TM\$(15,13)=TM\$(13,15)  
TM\$(15,14)=TM\$(14,15)  
TM\$(15,15)=-.5\*(B3\*B3+C3\*C3)\*CONST2

C

C

C

```
U(1)=U1
U(2)=U2
U(3)=U3
U(4)=U4
U(5)=U5
U(6)=U6
V(1)=V1
V(2)=V2
V(3)=V3
V(4)=V4
V(5)=V5
V(6)=V6
NT(1)=N1
NT(2)=N3
NT(3)=N5

QZ 00180
QZ 00190
QZ 00200
QZ 00210
QZ 00220
QZ 00230
QZ 00240
QZ 00250
QZ 00260
QZ 00270
QZ 00280
QZ 00290
QZ 00300
```

CC

```
CONST3=1./DEL*4.*60.
QZ1(1,1)=0.0
QZ1(2,1)=56.*(B2*C1-B1*C2)*CONST3
QZ1(2,2)=0.0
QZ1(3,1)=-8.*(B2*C1-B1*C2)*CONST3
QZ1(3,2)=12.*(B2*C1-B1*C2)*CONST3
QZ1(3,3)=0.0
QZ1(4,1)=12.*(B3*C1+B2*C2-B1*C3-B1*C2)*CONST3
QZ1(4,2)=16.*(B2*C1-B1*C2)+32.*(B3*C2+B3*C1-B2*C3-B1*C3)*CONST3
QZ1(4,3)=12.*(B3*C2-B2*C3)*CONST3
QZ1(4,4)=0.0
QZ1(5,1)=-8.*(B3*C1-B1*C3)*CONST3
QZ1(5,2)=-4.*(B3*C2-B2*C3)*CONST3
QZ1(5,3)=12.*(B3*C2-B2*C3)*CONST3
QZ1(5,4)=0.0
QZ1(6,1)=56.*(B3*C1-B1*C3)*CONST3
QZ1(6,2)=96.*(B3*C2-B2*C3)+32.*(B1*C2+B3*C1-B2*C3-B1*C3)*CONST3
QZ1(6,3)=-4.*(B1*C2-B2*C3)*CONST3
QZ1(6,4)=16.*(B1*C3-B3*C1)+32.*(B3*C2+B1*C2-B2*C3-B2*C1)*CONST3
QZ1(6,5)=12.*(B1*C3-B3*C1)*CONST3
QZ1(6,6)=0.0
QZ2(1,1)=0.0
QZ2(2,1)=12.*(B2*C1-B1*C2)*CONST3
QZ2(2,2)=0.0
QZ2(3,1)=-8.*(B2*C1-B1*C2)*CONST3
QZ2(3,2)=56.*(B2*C1-B1*C2)*CONST3
QZ2(3,3)=0.0
QZ2(4,1)=-8.*(B3*C1-B1*C3)-4.*(B2*C1-B1*C2)*CONST3

QZ 00340
QZ 00350
QZ 00360

QAR00030
QAR00040
QAR00050
QAR00060
QAR00070
QAR00080
QAR00090
QAR00100
QAR00110
QAR00120
QAR00130
QAR00140
QAR00150
QAR00160
QAR00170
QAR00180
QAR00190
QAR00200
QAR00210
QAR00220
QAR00230
QAR00240
QAR00250
QAR00260
QAR00270
QAR00280
QAR00290
QAR00300
```

```

QZ2(4,2)=(96.*(B3*C1-B1*C3)+32.*(B2*C1+B3*C2-B1*C2-B2*C3))*CONST3
QZ2(4,3)=56.*(B3*C2-B2*C3)*CONST3
QZ2(4,4)=0.0
QZ2(5,1)=-4.*(B3*C1-B1*C3)*CONST3
QZ2(5,2)=-4.*(B3*C2-B2*C3)-8.*(B3*C1-B1*C3))*CONST3
QZ2(5,3)=-8.*(B3*C2-B2*C3)*CONST3
QZ2(5,4)=-12.*(B3*C2-B2*C3)*CONST3
QZ2(5,5)=0.0
QZ2(6,1)=12.*(B3*C1-B1*C3)*CONST3
QZ2(6,2)=16.*(B1*C2-B2*C1)+32.*(B3*C1+B3*C2-B1*C2-B2*C3))*CONST3
QZ2(6,3)=12.*(B1*C2+B3*C2-B2*C1-B2*C3)*CONST3
QZ2(6,4)=16.*(B1*C2-B2*C3)+32.*(B1*C3+B1*C2-B3*C1-B2*C1))*CONST3
QZ2(6,5)=12.*(B1*C3-B3*C1)*CONST3
QZ2(6,6)=0.0
QZ3(1,1)=0.0
QZ3(2,1)=12.*(B2*C1-B1*C2)*CONST3
QZ3(2,2)=0.0
QZ3(3,1)=-4.*(B2*C1-B1*C2)*CONST3
QZ3(3,2)=12.*(B2*C1-B1*C2)*CONST3
QZ3(3,3)=0.0
QZ3(4,1)=-4.*(B3*C1-B1*C3)-8.*(B2*C1-B1*C2))*CONST3
QZ3(4,2)=16.*(B3*C2-B2*C3)+32.*(B2*C1+B3*C1-B1*C2-B1*C3))*CONST3
QZ3(4,3)=12.*(B3*C2-B2*C3)*CONST3
QZ3(4,4)=0.0
QZ3(5,1)=-8.*(B3*C1-B1*C3)*CONST3
QZ3(5,2)=12.*(B3*C2-B2*C3+B3*C1-B1*C3))*CONST3
QZ3(5,3)=-8.*(B3*C2-B2*C3)*CONST3
QZ3(5,4)=56.*(B3*C2-B2*C3)*CONST3
QZ3(5,5)=0.0
QZ3(6,1)=12.*(B3*C1-B1*C3)*CONST3
QZ3(6,2)=16.*(B3*C1-B1*C3)+32.*(B1*C2+B3*C2-B2*C1-B2*C3))*CONST3
QZ3(6,3)=-8.*(B1*C2-B2*C1)-4.*(B3*C2-B2*C3)*CONST3
QZ3(6,4)=-96.*(B1*C2-B2*C1)+32.*(B3*C2+B1*C3-B2*C3-B3*C1))*CONST3
QZ3(6,5)=56.*(B1*C3-B3*C1)*CONST3
QZ3(6,6)=0.0

```

C C

```

DO 57 JA=1,14
DO 57 JB=1,3
ICHECK=NT(JB)-NI(JA)
IF(ICHECK.EQ.0) GO TO 58
GO TO 57
IF(JB-2) 60,70,80
QPRM=0.0
DO 61 KO=1,6
DO 61 KM=1,KO
QPRM=QPRM+(U(KO)*V(KM)-U(KM)*V(KO))*QZ1(KO,KM)
CONTINUE

```

58 60 61

```

70 Q(NCP(NT(JB)))=QPRM+Q(NCP(NT(JB)))
   GO TO 57
   QPRM=0.0
   DO 71 KN=1,6
   DO 71 KL=1,KN
   QPRM=QPRM+(U(KN)*V(KL)-U(KL)*V(KN))*QZ2(KN,KL)
   CONTINUE
71 Q(NCP(NT(JB)))=QPRM+Q(NCP(NT(JB)))
   GO TO 57
80 CERM=0.0
   DO 81 KP=1,6
   DO 81 KQ=1,6
   QPRM=QPRM+(U(KP)*V(KQ)-U(KQ)*V(KP))*QZ3(KP,KQ)
   CONTINUE
81 Q(NCP(NT(JB)))=QPRM+Q(NCP(NT(JB)))
57 CONTINUE
   QZC(1)=C1*C1
   QZC(2)=2.*C1*C2
   QZC(3)=C2*C2
   QZC(4)=2.*C2*C3
   QZC(5)=C3*C3
   QZC(6)=2.*C1*C3
   QZB(1)=B1*B1
   QZB(2)=2.*B1*B2
   QZB(3)=B2*B2
   QZB(4)=2.*B2*B3
   QZB(5)=B3*B3
   QZB(6)=2.*C1*C3
   NLCY(1)=17
   NLCY(2)=18
   NLCY(3)=20
   NLCY(4)=22
   NRCY(1)=30
   NRCY(2)=33
   NRCY(3)=34
   NRCY(4)=36
   CONST4=A/(4.*DEL**2)
   DO 513 LA=1,4
   JCHECK=K-NLCY(LA)
   KCHECK=K-NRCY(LA)
   IF(JCHECK.EQ.0) GO TO 517
   IF(KCHECK.EQ.0) GO TO 519
   GO TO 513
517 THETA=ATAN((YC(NT(3))-YC(NT(2)))/(XC(NT(3))-XC(NT(2))))
   THETA1=THETA-2.*ATAN(1.)
   SLIJ=SQRT((YC(NT(3))-YC(NT(2)))**2+(XC(NT(3))-XC(NT(2)))**2)
   XHAT=COS(THETA1)
   YHAT=SIN(THETA1)

```

QZ 00550  
QZ 00560  
QZ 00570  
QZ 00580  
QZ 00590

QZ 00630  
QZ 00640  
QZ 00650

GO 00020  
GO 00030  
GO 00040  
GO 00050  
GO 00060  
GO 00070  
GO 00080  
GO 00090  
GO 00100  
GO 00110  
GO 00120  
GO 00130  
GO 00140  
GO 00150  
GO 00160  
GO 00170  
GO 00180

```

PART1=0.0
PART2=0.0
TPART=0.0
DO 523 LB=1,6
PART1=PART1+(U(LB)*QZB(LB))*CONST4
PART2=PART2+(V(LB)*QZC(LB))*CONST4
CONTINUE
TPART=PART1+PART2
Q(NCP(NT(2)))=Q(NCP(NT(2)))+TPART*SLIJ
Q(NCP(NT(3)))=Q(NCP(NT(3)))+TPART*SLIJ
GC TO 513
523
THETA2=ATAN((YC(NT(1)))-YC(NT(2)))/(XC(NT(2))-XC(NT(1))))
THETA1=6.*ATAN(1.)-THETA2
SLIJ=SQRT((YC(NT(1)))-YC(NT(2)))*2+(XC(NT(1)))-XC(NT(2)))*2)
XHAT=COS(THETA1)
YHAT=SIN(THETA1)
TPART=0.0
PART1=0.0
PART2=0.0
DO 521 LB=1,6
PART1=PART1+(U(LB)*QZB(LB))*CONST4
PART2=PART2+(V(LB)*QZC(LB))*CONST4
CONTINUE
TPART=PART1+PART2
Q(NCP(NT(1)))=Q(NCP(NT(1)))+TPART*SLIJ
Q(NCP(NT(2)))=Q(NCP(NT(2)))+TPART*SLIJ
CONTINUE
CONTINUE
N(1)=N1
N(2)=N2
N(3)=N3
N(4)=N4
N(5)=N5
N(6)=N6
N(7)=N7
N(8)=N8
N(9)=N9
N(10)=N10
N(11)=N11
N(12)=N12
N(13)=N13
N(14)=N14
N(15)=N15
DO 200 I$=1,15
I= N(I$)
DO 200 J$=1,15
J= N(J$)
TM(I,J)=TM(I,J)+TM$(I$,J$) .
519
521
513
185

```

```

GO 00210
GO 00220
GO 00240
GO 00250
GO 00260
GO 00270
GO 00280
GO 00290
GO 00300
GO 00320
FLU04470
FLU04480
FLU04490
FLU04500
FLU04510
FLU04520
FLU04530
FLU04540
FLU04550
FLU04560
FLU04570
FLU04580
FLU04590
FLU04600
FLU04610
FLU04620
FLU04630
FLU04640
FLU04650
FLU04660
FLU04670

```



```

200 CONTINUE
300 CONTINUE
   IF(NNQXY.EQ.0) GO TO 310
   DO 310 I=1,NNQXY
     RHS(NQS(I))=RHS(NQS(I))+Q(NQS(I))
     RHS(NQS(I)+NN)=RHS(NQS(I)+NN)+Q(NQS(I)+NN)
   IF(I-NNPQ)309,309,310
309 RHS(NCP(NPS(I+NNPS)))=RHS(NCP(NPS(I+NNPS)))+Q(NCP(NPS(I+NNPS)))
310 CONTINUE
320 CONTINUE
   CALL SOLMIX(MM,IM,T,RHS,NTOTVP,NVIS,NTOTQ,NQIS,B,Z,C)
   WRITE(NWRITE,2000)
   NTEST=0
   DO 322 J=1,MM
     ESPILA=ABS(T1(J)-T(J))
     IF(ESPILA-.001)322,324,324
322 CONTINUE
324 NTEST=100
   DO 325 I=1,NN
     IV=I+NN
     IQ=I+2*NN
     T1(I)=
       T(I)
     Q(I)=RHS(I)
     T1(IV)=
       T(IV)
     Q(IV)=RHS(IV)
     IF(MM-IQ)2223,2222,2222
     T1(IQ)=
       T(IQ)
     Q(IQ)=RHS(IQ)
   WRITE(NWRITE,2300)I,T(I),IV,T(IV),IQ,T(IQ),Q(I),Q(IV),Q(IQ)
   GC TO 325
2223 WRITE(NWRITE,2301)I,T(I),IV,T(IV),Q(I),Q(IV)
325 CONTINUE
   IF(NTEST.NE.100) GO TO 177
500 FORMAT(110)
1005 FORMAT(6X,A4,I10,2F10.0)
1006 FORMAT(6X,A4,I10,2F10.0)
1010 FORMAT(7110)
1015 FORMAT(6X,A4,I10,F10.0)
1016 FORMAT(6X,A4,I10,F10.0)
1020 FORMAT(110,2F10.0)
1025 FORMAT(6X,A4,I10,F10.0)
1030 FCFORMAT(6X,A4,2I10,2F10.0)
1035 FORMAT(5X,'NO. OF CORNER NODES=',I3,/,
15X,'NO. OF SUMMARY OF NODAL COORDINATES',/,
17X,'I',I,12X,'X(I)',I2X,'Y(I)',/,
1045 FORMAT(5X,I3,2(7X,F10.3))

```

FLU04680  
 FLU04690  
 FLU04700  
 FLU04710  
 FLU04720  
 FLU04730

FLU04740  
 FLU04750  
 FLU04760  
 FLU04770

FLU04780  
 FLU04790  
 FLU04800  
 FLU04810

FLU04820

FLU04860

FLU04880  
 FLU04890  
 FLU04900  
 FLU04910  
 FLU04920  
 FLU04930  
 FLU04940  
 FLU04950  
 FLU04960  
 FLU04970  
 FLU04980  
 FLU04990  
 FLU05000  
 FLU05010

```

1050 FORMAT(5X,'LISTING OF SYSTEM TOPOLOGY',//,5X
1,ELEMENT NUMBER',20X,'NODE NUMBERS',//)
1055 FORMAT(5X,I3,10X,6(5X,I3))
1060 FORMAT(7X,'NODES WHERE VELOCITIES ARE SPECIFIED',
//,8X,I1,5X,'NODE',5X,'U VELOCITY',5X,'V VELOCITY',//)
1065 FORMAT(2X,2(4X,I3),3X,F12.3,3X,F12.3)
1070 FORMAT(5X,'SPECIFIED RIGHT HAND SIDE I.E. QX AND QY',
//,2X,'NODE',5X,'QX',5X,'QY',//)
1071 FORMAT(5X,'SPECIFIED RIGHT HAND SIDE FOR PRESSURE NODES, I.E. QZ',
//,2X,'NODE',5X,'QZ',//)
1072 FORMAT(2X,2(4X,I3),3X,F12.3)
1075 FORMAT(5X,I3,2(10X,F12.3))
1080 FORMAT(5X,'NODES WHERE PRESSURE IS SPECIFIED',
//,5X,I1,5X,'NODE',10X,'PRESSURE',//)
1085 FORMAT(5X,I3,3X,I3,10X,F12.3)
2300 FORMAT(6X,3(I3,5X,E13.5,5X),3(E13.5,3X))
2301 FORMAT(6X,2(I3,5X,E13.5,5X),26X,2(E13.5,3X))
2000 FORMAT(3X,'NODE NO.',3X,'T(I)',5X,'X-COORD',5X,'NODE NO.',2X,'T(J)',2
1X,'Y-COORD',5X,'NODE NO.',4X,'T(I)',9X,'Q(I)' X',17X,'Q(I)' Y',12
2X,'Q(I)' P')
2020 FORMAT(1H1,5X,'THIS IS A NON-LINEAR PROBLEM',//)
STOP
END

```

FLU0505020  
 FLU0505030  
 FLU0505040  
 FLU0505050  
 FLU0505060  
 FLU0505070  
 FLU0505080  
 FLU0505090  
 PRE00200  
 PRE00210  
 PRE00220  
 FLU05100  
 FLU05110  
 FLU05120  
 FLU05130

FLU05210  
 FLU05220  
 FLU05230

```

SUBROUTINE SOLMIX(N,A,X,Y,NX,LISTX,NY,LISTY,B,Z,C)
DIMENSION A(N,N),X(N),Y(N),Z(NY),C(NY)
IF(N.EQ.(NX+NY)) GO TO 100
WRITE(6,111) N,NX,NY
FORMAT(10X,'N=',I2,10X,'NX=',I2,10X,'NY=',I2)
111 STOP
100 CONTINUE
IF(NX.NE.0) GO TO 120
CALL SOLVE(N,A,Y,X)
RETURN
120 CONTINUE
IF(NY.NE.0) GO TO 140
DO 130 I=1,N
Y(I)=0.
DO 130 J=1,N
Y(I)=Y(I)+A(I,J)*X(J)
130 Y(I)=Y(I)+A(I,J)*X(J)
140 CONTINUE
DO 200 I=1,NY
DO 200 J=1,NY
B(I,J)=A(LISTY(I),LISTY(J))
DO 300 I=1,NY
C(I)=Y(LISTY(I))
DO 300 J=1,NX
C(I)=C(I)-A(LISTY(I),LISTX(J))*X(LISTX(J))
CALL SOLVE(NY,B,C,Z)
DO 400 I=1,NY
X(LISTY(I))=Z(I)
DO 800 I=1,NX
C(I)=0.
DO 600 J=1,NY
C(I)=C(I)+A(LISTX(I),LISTY(J))*X(LISTY(J))
DO 700 J=1,NX
C(I)=C(I)+A(LISTX(I),LISTX(J))*X(LISTX(J))
800 Y(LISTX(I))=C(I)
RETURN
END

```

SOL000010  
SOL000020  
SOL000030  
SOL000040  
SOL000050  
SOL000060  
SOL000070  
SOL000080  
SOL000090  
SOL000100  
SOL000110  
SOL000120  
SOL000130  
SOL000140  
SOL000150  
SOL000160  
SOL000170  
SOL000180  
SOL000190  
SOL000200  
SOL000210  
SOL000220  
SOL000230  
SOL000240  
SOL000250  
SOL000260  
SOL000270  
SOL000280  
SOL000290  
SOL000300  
SOL000310  
SOL000320  
SOL000330  
SOL000340  
SOL000350  
SOL000360  
SOL000370  
SOL000380  
SOL000390

```

SUBROUTINE SOLVE(N,A,C,X)
  DATA NWRITE/6/
  DIMENSION A(N,N),X(N),C(N)
  DO 400 K=1,N
    BIG = ABS(A(K,K))
    IBIG = K
    DO 100 I=K,N
      SIZE = ABS(A(I,K))
      IF(SIZE.LT.BIG) GO TO 100
    BIG=SIZE
    IBIG=I
  100 CONTINUE
    IF(K.EQ. IBIG) GO TO 280
    DO 200 J=K,N
      ABIG = A(IBIG,J)
      A(IBIG,J)=A(K,J)
    200 A(K,J)= ABIG
      CBIG = C(IBIG)
      C(K)=CBIG
    280 CONTINUE
    IF(A(K,K).EQ.0.) GO TO 600
    DO 350 I=1,N
      IF(I.EQ.K) GO TO 350
      RATIO = A(I,K)/A(K,K)
      DO 300 J=K,N
        A(I,J)=A(I,J)-RATIO*A(K,J)
      A(I,J)=A(I,J)-RATIO*A(K,J)
      CALL OVERFL(IQ)
      IF(IQ.EQ.2)GO TO 301
      WRITE(6,98)
    98 FORMAT(1X,IQ,I,J,K,A(I,J),A(K,J),RATIO,A(K,J)
    99 FORMAT(1X,4I5,3E15.6)
      IF(IQ=1) OVERFLOW.....IQ=3 UNDERFLOW
    301 CONTINUE
    300 C(I) = C(I) -RATIO*C(K)
    350 CONTINUE
    400 CONTINUE
    DO 500 K=1,N
      X(K) = C(K)/A(K,K)
    500 RETURN
    600 WRITE(6,666)
    666 FORMAT(10X,'SINGULAR MATRIX')
    700 X(I)=0.
    2 WRITE(NWRITE,2)K
      FORMAT(6X,'K=',I5)

```

```

SOL00010
SOL00020
SOL00030
SOL00040
SOL00050
SOL00060
SOL00070
SOL00080
SOL00090
SOL00100
SOL00110
SOL00120
SOL00130
SOL00140
SOL00150
SOL00160
SOL00170
SOL00180
SOL00190
SOL00200
SOL00210
SOL00220
SOL00230
SOL00240
SOL00250
SOL00260

```

RATIO')

```

SOL00270
SOL00280
SOL00290
SOL00300
SOL00310
SOL00320
SOL00330
SOL00340
SOL00350
SOL00360

```

## BIBLIOGRAPHY

1. Kenneth H. Huebner, The Finite Element Method for Engineers, Wiley, 1975.
2. Office of Naval Research, PROJECT SQUID, by W.H.Stevenson and H.D.Thompson, 9-10 March 1972.
3. C. Taylor and P. Hood, "A Numerical Solution of the Navier-Stokes Equations Using the Finite Element Technique", Computers Fluids, Vol. I, No. 1, 1973.
4. 30<sup>th</sup> Annual National Forum of the American Helicopter Society, Laser Velocimeter Measurements of the Helicopter Rotor Induced Flow Field, by J.C. Biggers and K.L. Orlaff, May 7-9, 1974.



# INITIAL DISTRIBUTION LIST

	No. Copies
1. Defense Documentation Center Cameron Station Alexandria, Virginia 22314	2
2. Library, Code 0212 Naval Postgraduate School Monterey, California 93940	2
3. Department Chairman, Code 57 Department of Aeronautics Naval Postgraduate School Monterey, California 93940	1
4. Professor D. J. Collins, Code 57Co Department of Aeronautics Naval Postgraduate School Monterey, California 93940	1
5. LT Terry Scott Wanner, USN 6414 W. Wicklow Circle Colorado Springs, Colorado 80907	1
6. Dr. H. J. Mueller Code 310 Naval Air Systems Command Washington, D. C. 20361	1

thesW227

Laser doppler anemometer measurement and



3 2768 001 92949 0

DUDLEY KNOX LIBRARY